Journal of Neuromorphic Intelligence

REVIEW ARTICLE

VOLUME 03 | MARCH 2026

Flexible Biosensors for Health Monitoring in the Era of AI: Design, Fabrication, and Edge Intelligence

Prashant Dhakal[1], Aolin Hou[2], Jae Gwang Kim[2], Xiaofei Wu[1], Jingjing Qiu[3] ,Shiren Wang[1,2,*]

1 Department of Industrial and Systems Engineering, Texas A&M University, College Station, TX, USA
2 Department of Material Science and Engineering, Texas A&M University, College Station, TX, USA
3 Department of Mechanical Engineering, Texas A&M University, College Station, TX, USA
** Corresponding author: s.wang@tamu.edu*

ABSTRACT

Flexible and wearable biosensors, when co-designed with artificial intelligence, enable continuous health monitoring by converting noisy, motion-corrupted physiological signals into reliable clinical information. This review summarizes key flexible modalities (ECG, PPG/SpO_2,cuffless blood pressure, temperature, and biochemical sensing), materials and mechanical layouts, and scalable fabrication strategies, and explains how these choices shape signal quality, robustness, and suitability for edge and neuromorphic AI. It further outlines a design-for-AI framework that co-optimizes sensor placement, mechanics, and sampling with lightweight edge models, multimodal fusion, and federated learning to realize low-power, privacy-preserving, and equitable wearable health systems.

Keywords: ***Flexible biosensors, wearable health monitoring, edge AI, design-for-AI, multimodal physiological sensing, stretchable electronics, machine learning***

1. INTRODUCTION

Flexible and wearable biosensors have emerged as a promising platform for continuous health monitoring because they can conform to soft, curved, and dynamically moving biological surfaces while enabling real-time acquisition of physiological signals. Compared with conventional rigid devices, skin-interfaced and mechanically compliant sensors offer improved comfort, intimate contact with the body, and greater potential for long-term use in daily life. Early advances in epidermal electronics established the feasibility of ultrathin, skin-like sensor systems, while subsequent work demonstrated low-cost electronic tattoos and multifunctional wearable patches capable of monitoring signals such as electrocardiogram (ECG), temperature, motion, and biochemical markers[1-4]. These developments have accelerated the transition from intermittent, clinic-based measurements toward personalized and continuous monitoring in ambulatory and home settings. At the same time, the practical value of flexible biosensors depends not only on the ability to collect data, but also on the ability to convert noisy, high-volume, and multimodal signals into clinically meaningful information. In real-world use, wearable signals are frequently degraded by motion artifacts, inconsistent skin contact, environmental interference, and substantial inter-subject variability. These challenges make artificial intelligence (AI) and machine learning (ML)

Received: 11 Janurary 2026

Accepted: 22 Feburary 2026

Published: 9 March 2026

Check for updates

increasingly important for robust signal interpretation, artifact-tolerant feature extraction, classification, regression, and prediction. The growing impact of AI in wearable health monitoring is reflected both in broad reviews of ML-enabled wearable systems and in influential demonstrations such as deep-learning-based arrhythmia detection from ambulatory ECGs[4-6]. Accordingly, flexible biosensors should be viewed not simply as data acquisition tools, but as front-end systems whose material selection, mechanical design, modality choice, and sampling strategy directly affect downstream model performance.

This review therefore examines flexible biosensors for vital-sign monitoring from a combined device design, fabrication, and AI-integration perspective, with particular emphasis on a "designed for AI" framework. We first summarize major flexible sensing modalities relevant to physiological monitoring, including ECG, photoplethysmography (PPG)/ peripheral capillary oxygen saturation (SpO_2), cuffless blood-pressure surrogate sensing, temperature sensing, and other physiological or biochemical channels that can serve as auxiliary inputs for intelligent models. We then discuss the materials, mechanical architecture, and fabrication strategies that determine signal quality, wearability, and manufacturability. Building on this foundation, we review signal-processing and AI/ ML methods for transforming raw bio-signals into actionable health information, while highlighting how hardware-level design choices influence algorithmic accuracy, robustness, and deployment constraints. Finally, we discuss emerging opportunities in edge and neuromorphic intelligence, where sensing, computation, and decision-making may be pushed closer to the body to reduce latency, bandwidth demand, and power consumption[4, 7, 8]. By linking flexible sensor engineering with downstream computational requirements, this review aims to clarify how next-generation wearable systems can be intentionally designed not only to acquire physiological data, but also to produce data that are maximally useful for intelligent health monitoring

2. FLEXIBLE BIOSENSOR MODALITIES FOR VITAL SIGNS

Flexible vital-sign sensors are designed not only to detect physiological signals, but also to maintain stable contact with soft, moving skin. Across recent studies, performance depends on coordinated choices in materials, mechanics, and signal transduction, which is why recent systems increasingly combine electrical, optical, thermal, and mechanical channels in one wearable platform[7, 9, 10].

2.1 FLEXIBLE ECG SENSORS

Flexible ECG research has shifted from conventional wet electrodes toward dry, skin-conformal interfaces that better support long-term and ambulatory monitoring. Recent studies describe gel-less sticky patches, e-skin electrodes, and broader flexible dry-electrode platforms built from conductive polymers, carbon-based materials, and stretchable composites designed to reduce impedance while preserving comfort and adhesion (Figure 1). Across these studies, three requirements dominate: intimate skin contact, motion robustness, and stable waveform quality. Yamamoto et al.[9] show that electrode composition and contact area affect impedance and R-wave attenuation, whereas Hao et al.[10] demonstrate clear ECG recording under sweat, deformation, and dynamic activity through a breathable, self-adhesive design. Overall, flexible ECG performance depends less on conductivity alone than on a mechanically persistent, low-impedance skin-electrode interface. This emphasis on stable skin contact carries directly into optical sensing, where conformal wear is essential but the main design constraints shift toward light transport, wavelength choice, and site-dependent signal quality.

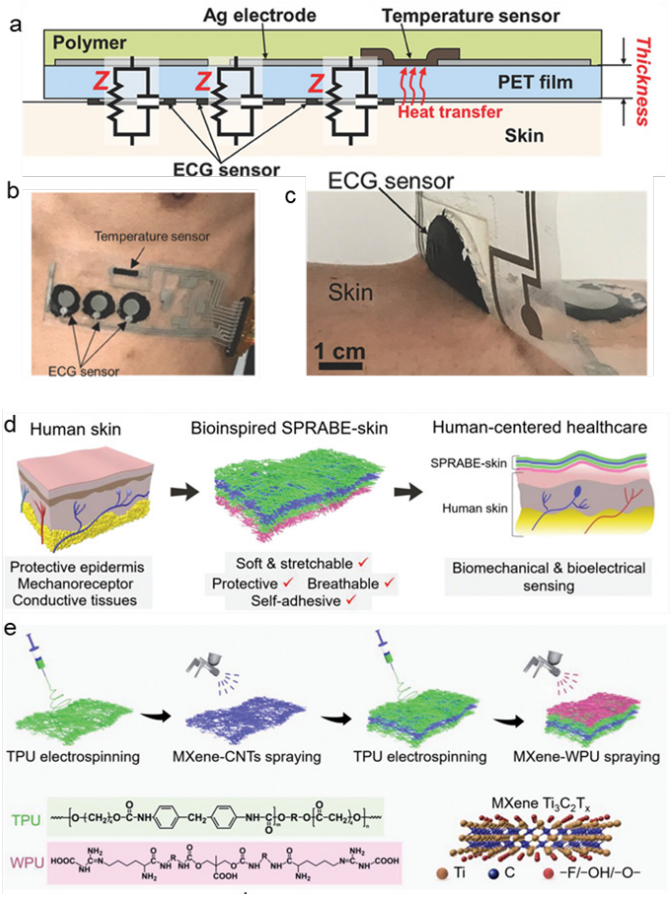


Figure 1: a) Schematic image of the equivalent circuit of the ECG sensor and heat transfer through a PET film from skin to the device[9]. b) Photo of the fabricated device. c) Photo of the adhesion test of the device peeled from skin. The design of the bioinspired E-skin (SPRABE). d) Schematic illustration of the bioinspired design of SPRABE-skin[10]. e) Fabrication process of the SPRABE-skin based on electrospinning and spraying (top). Adopted with permission[9], © 2017 WILEY-VCH Verlag GmbH & Co. KGaA, Weinheim.

2.2 FLEXIBLE PPG/SPO_2 SENSORS

Flexible PPG and SpO_2 sensors monitor pulsatile blood-volume changes optically, and the current research shows that their design is governed by both optical layout and wearable mechanics. Reflective systems place the emitter and detector on the same side of the tissue, whereas transmissive systems place them on opposite sides. These choices shape wavelength selection, power demand, and usable body sites[11] (Figure 2 a-e). Multi-wavelength designs further expand the physiological information that can be extracted

from a single platform12 (Figure 2f,g). The main trade-off is between signal quality and wearability. Finger-based configurations generally provide stronger optical signals, while wrist-mounted devices are easier to wear continuously but are more vulnerable to motion artifacts. The current studies therefore converge on compliant packaging, stretchable interconnects, and site-specific optical design as key strategies for preserving signal quality in daily use. Once PPG is treated as more than a heart-rate signal and instead as a waveform rich in timing and morphology, it becomes a natural input for cuffless blood-pressure estimation.

2.3 CUFFLESS BLOOD PRESSURE (BP) SURROGATE SENSORS

Research has presented cuffless blood-pressure monitoring as a multimodal inference problem rather than a direct one-sensor measurement. Major surrogate routes include PPG plus timing metrics such as pulse arrival time (PAT) or pulse transit time (PTT), pulse-wave analysis, soft pressure or tonometric sensing, and bioimpedance-based approaches that probe arterial dynamics through tissue electrical properties[7, 13]. Among the recent studies, the clearest PPG-based example is a wearable flexible wrist patch that combines PPG with ECG timing and Kalman filtering for blood-pressure estimation[14]. Furthermore, recent reviews emphasize that PPG is not the sole solution. Soft pressure sensors and ring-type bioimpedance devices provide vital surrogates that may be more reliable under certain conditions. Specifically, the development of bioimpedance rings illustrates the critical role of electrode configuration in overcoming skin-tone sensitivity and improving overall device robustness[15](Figure a-e). These BP surrogates also show why auxiliary sensing channels matter: they provide context that can help separate true cardiovascular changes from environmental or motion-related variation.

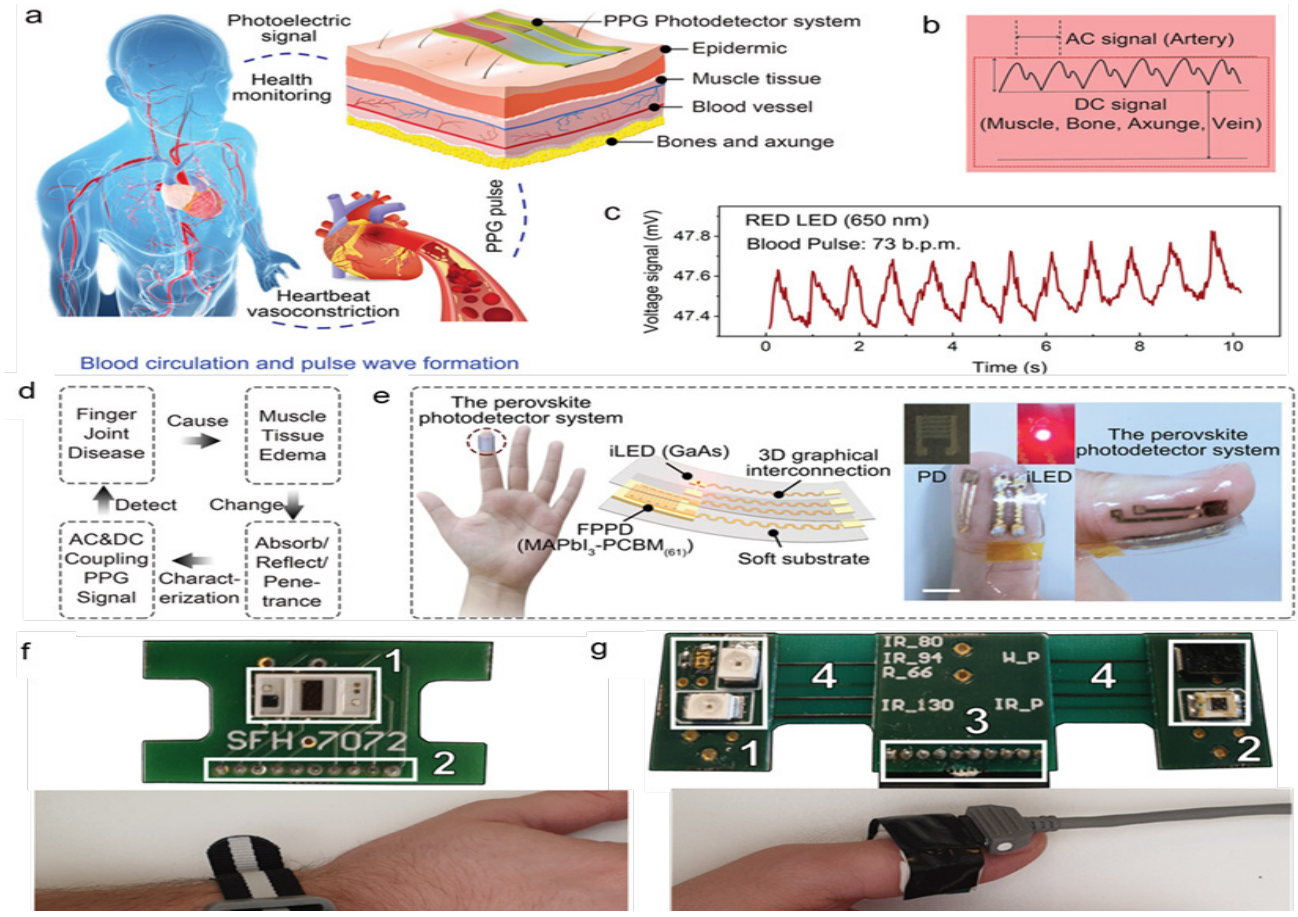


Figure 2: a) Schematic diagram of the working principle of the cardiovascular cerebrovascular circulatory system of the human body and the photoplethysmography (PPG) signal sensing applied to the surface of human skin11. b) The basic curve structure of PPG signal and the response structure of different parts from subcutaneous tissue. c) The PPG signal read within 10 s (wavelength: 650 nm). g) Schematic of the swelling detection by variable PPG signal. h) The detailed structure diagram and physical schematic of the flexible PPG signal sensor (inset: Left: flexible perovskite photodetector; right: red led used as light source). Scale bar: 0.5 cm. f) The inner PCB and fully assembled wrist probe12. g) The finger probe design utilizes the semi-flex PCB technology to accommodate various finger sizes. Adopted with permission [3] , © 2023 Wiley VCH GmbH. Reprinted with permission [4] , Creative Commons Attribution 4.0 (CC BY 4.0), https://creativecommons.org/licenses/by/4.0/.

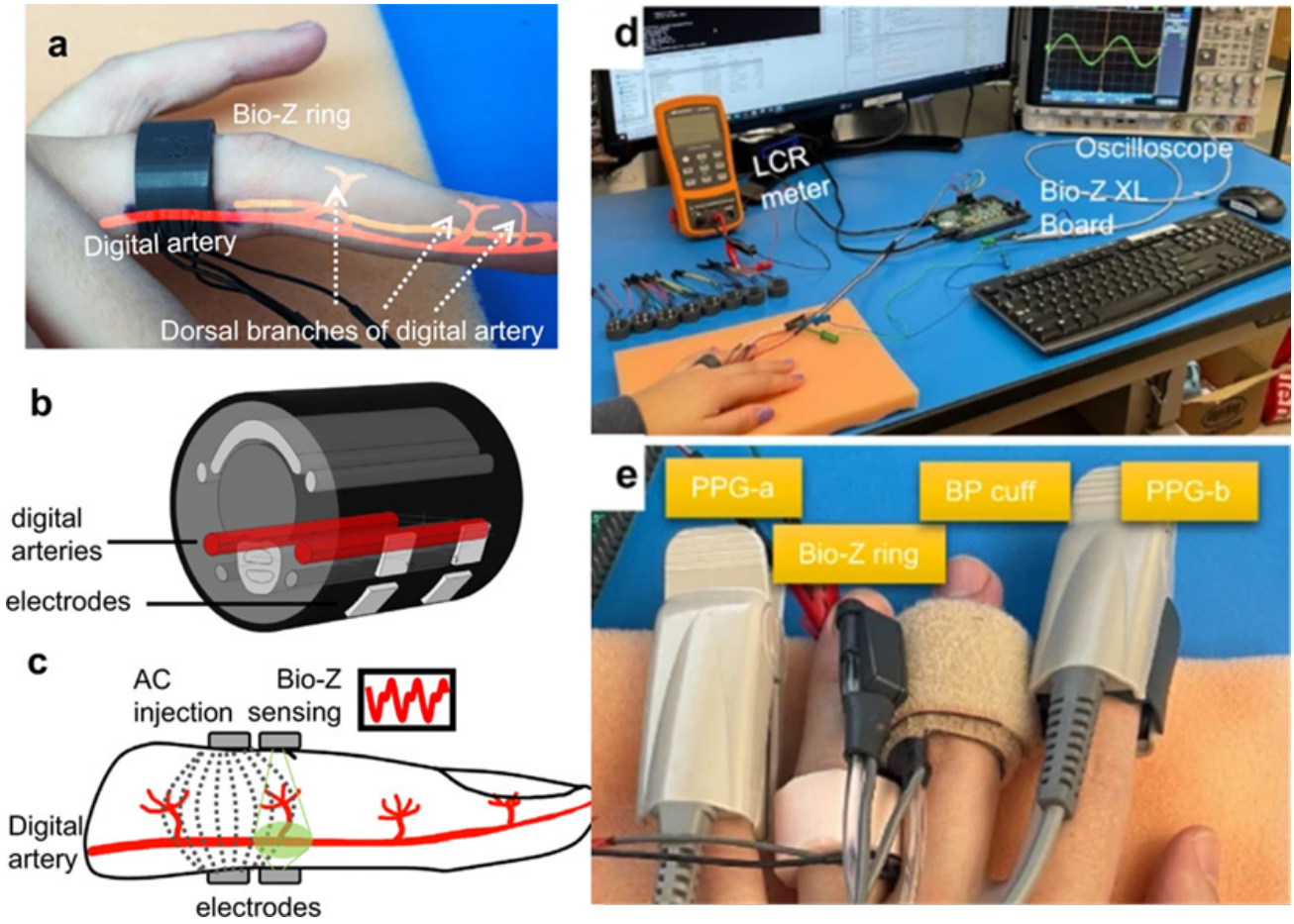


Figure 3: a) A fabricated ring example custom fit to user's finger size15. b) The finite element model of the human finger used in guiding ring design. c) Cross-section of the four electrode bioimpedance sensing, with dashed lines representing high frequency alternating current (AC) distribution within the finger, and green area shows sensitive area for Bio-Z sensing electrodes. d) Experimental setup used in assessing bioimpedance signal quality acquired with ring sensors. e) Different sensors on the same hand are used for BP experiments. Reprinted with permission [5] , Creative Commons Attribution 4.0 (CC BY 4.0), https://creativecommons.org/licenses/by/4.0/.

2.4 TEMPERATURE AND OTHER PHYSIOLOGICAL/BIOCHEMICAL SENSORS

Temperature, sweat, strain, and respiration-related sensors expand the physiological information that wearable systems can capture and therefore strengthen signal interpretation. Yamamoto et al.[9] demonstrated that the accuracy of thin-film skin-temperature sensing is strongly influenced by substrate thickness, with thinner PET films providing more reliable temperature readouts. They also integrated temperature and ECG sensing into a single wearable patch. In parallel, flexible sweat sensors have enabled electrochemical detection of ions and metabolites, while multimodal e-skin devices have shown that strain-related signals can be monitored together with cardiovascular signals[16, 17].

These auxiliary channels are particularly important for AI-enabled wearables because they provide contextual variables that reduce ambiguity in signal interpretation. Temperature informs changes in perfusion and optical coupling, strain and respiration reflect posture and motion state, and sweat chemistry provides insight into hydration, electrolyte balance, and metabolic status. Accordingly, auxiliary sensing should be regarded as an essential design component of interpretable, personalized multimodal platforms rather than a secondary addition.

3. MATERIALS AND MECHANICAL DESIGN FOR FLEXIBLE BIOSENSORS

The performance of flexible biosensors is governed not only by the transduction mechanism, but also by how materials, interfaces, and structural layouts work together under repeated deformation and prolonged skin contact. Successful wearable biosensors are built by co-optimizing substrate mechanics, conductive/optoelectronic functionality, and device architecture, rather than treating these elements as independent design choices[18-20].

3.1 SUBSTRATES AND ENCAPSULATION

Substrates and encapsulation layers define the first-order interface between the device, the body, and the external environment. In the recent literature, the central design tension is no longer simply flexibility versus rigidity, but the more demanding balance among conformability,

breathability, environmental protection, and long-term wearability. Three substrate directions recur across recent studies: elastomeric films, textile-derived platforms, and ultrathin or substrate-free membranes. Stretchable on-skin substrates can be classified mainly into elastomers/composites, kirigami-inspired structures, and textile engineering, while also emphasizing that breathable health-monitoring systems increasingly rely on porous or fibrous construction rather than continuous, impermeable films[19]. Textile platforms are attractive because their intrinsic void space enables rapid gas and water-vapor transport, while still offering softness, drapability, and body-scale integration; however, their rougher and more heterogeneous surfaces can complicate intimate electrode-skin contact. By contrast, ultrathin and substrate-free electrodes reduce bending stiffness and improve conformity to curved skin, which directly lowers motion artifacts and stabilizes signal collection over time[21, 22]. Figure 4 summarizes the fabrication route for free-standing conductive films and their use as ultra-conformal, breathable epidermal bioelectrodes. It supports the argument that ultrathin, substrate-free designs can combine conformality with gas permeability more effectively than conventional supported electrodes.

Encapsulation introduces a competing requirement: devices must resist sweat, humidity, oxygen, and abrasion without sacrificing softness. This remains difficult because low-modulus materials usually provide poor barrier performance, and that performance often degrades further under strain [18, 23]. The challenge is especially important for flexible organic optoelectronics that must remain stable while being laminated onto skin. Figure 5 plots water and oxygen barrier properties against elastic modulus for common flexible-sensor materials. It highlights the central encapsulation challenge in wearable biosensors: the softest materials are often the least effective barriers, so low-modulus encapsulation with strong environmental protection remains a major unmet need.

Long-term wear also requires breathable, biocompatible, and durable interfaces. Breathability reduces thermal discomfort and skin irritation, while adhesive layers must maintain contact without blocking gas exchange. Matsuhisa et. al.[23] emphasizes that meaningful evaluation depends on position and duration of tissue contact, with ISO 10993-type testing frameworks relevant for irritation, sensitization, and broader biological response. Adhesion must also be tuned carefully. Dong et. al.[19] identifies pressure-sensitive adhesives as promising because they can enhance skin contact without necessarily blocking gas or liquid permeability, but only when their viscoelasticity and composition are matched to the device stack. For textile or fabric-based systems, cleaning and moisture robustness become part of the packaging problem itself. In this direction, Sun et.al.[25] shows that hydrophobic outer protection can help prevent delamination and oxidation of conductive networks in highly humid or sweat-rich conditions, while washable breathable sensors demonstrate that maintenance durability must be treated as a functional requirement rather than an afterthought. Together, these studies show that future substrate and encapsulation design must deliver not only softness, but also safe, cleanable, and stable operation in daily use.

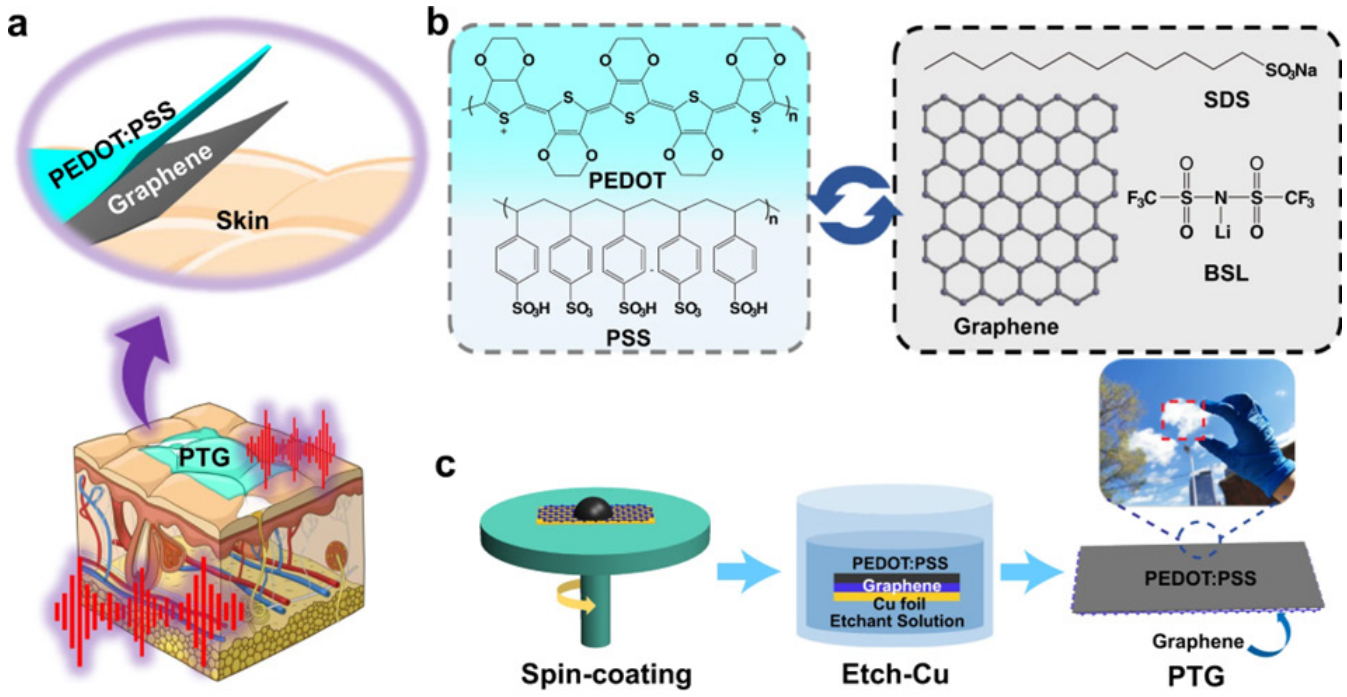


Figure 4: a Schematic illustration of PEDOT:PSS transferred CVD graphene film (PTG) as a skin electrode for electrophysiology22. b Chemical structure of PEDOT:PSS, graphene, sodium dodecyl sulfate (SDS), and bis(trifluoromethane) sulfonimide lithium salt (BSL). c Schematic illustration of the fabrication process of the double-layer stacked structure of PEDOT:PSS/graphene. Inset is a transparent PTG held on a plastic substrate. Reprinted with permission [6] , Creative Commons Attribution 4.0 (CC BY 4.0), https://creativecommons.org/licenses/by/4.0/.

3.2 CONDUCTIVE AND OPTOELECTRONIC MATERIALS

Once the substrate is selected, the next design layer is the set of active electrical and optical materials. Here, the research converges on a practical requirement: conductors, emitters, and detectors must retain performance under strain while remaining compatible with thin, low-temperature, and often solution-based fabrication routes suitable for wearable formats.

For conductors, there are two main strategies for materials design. The first is to use high-conductivity metal-based systems, often reformulated into deformable or porous forms. Tang et. al.[26] reports printable metal-polymer conductors with conductivity of 2316 S cm-1 at 500% strain and resistance change below 3% after 10,000 cycles, underscoring the exceptional electrical robustness achievable with liquid-metal-derived composites. The limitation is that these systems often need additional protection against leakage, oxidation, cracking, or delamination, particularly when integrated into thin on-skin patches. The second strategy is to rely on intrinsically softer conductors, especially conductive polymers, that better match the mechanics of skin-interfaced device[27].

Among conductive polymers, PEDOT:PSS is the most recurrent material because it can be printed, blended, and mechanically softened without abandoning useful conductivity. Lo et.al.[27] shows that adding ethylene glycol (EG) promotes PEDOT/PSS phase separation and structural rearrangement, improving charge transport through a more percolated PEDOT network; subsequent blending with PEO imparts stretchability, allowing the printed films to tolerate up to 50% tensile strain with relatively small electrical degradation. Figure 6 compares pristine PEDOT:PSS with EG-modified films and schematically links solvent-induced phase separation to improved hole transport. It supports the broader point that conductive-polymer performance in wearable biosensors is strongly governed by morphology engineering, not just nominal composition. What emerges across the PEDOT:PSS papers is a recurring compromise: additives that improve conductivity and additives that improve elasticity are not interchangeable, so wearable biosensor conductors are usually engineered around a targeted balance point rather than a single maximized property

For PPG and SpO_2 sensing, the materials problem shifts from simple conduction to coupled light emission and detection. Dcosta's review makes clear that all-organic pulse-oximetry platforms rely primarily on organic light-emitting diodes (OLEDs) or polymer light-emitting diodes as the light source and organic photodetectors (OPDs) as the detector, typically fabricated on ultrathin polyethylene naphthalate (PEN), polyethylene terephthalate (PET), or parylene-class substrates. These systems are attractive because organic semiconductors are lightweight, solution-processable, compatible with large-area flexible substrates, and more naturally suited to conformal body contact than conventional rigid silicon components. Current design trends favor reflective-mode PPG for wearables, with circular emitter-detector geometries providing superior performance over rectangular alternatives. Central to this design is the need for conformal contact, which mitigates motion artifacts and prevents optical crosstalk. Figure 7 illustrates a representative flexible organic PPG architecture[28]. It supports the point that wearable optical biosensors depend simultaneously on material stack design, mechanical flexibility, and anatomical placement.

3.3 DEVICE ARCHITECTURE AND MECHANICS

The mechanical reliability of flexible biosensors depends as much on structural layout as on material selection . Recent studies of stretchable hybrid electronics show that high-performance wearable systems are commonly built by placing rigid sensing or processing elements on low-strain regions and linking them through deformable interconnects, so that the applied strain is redirected away from fragile components[30]. This rigid–flex

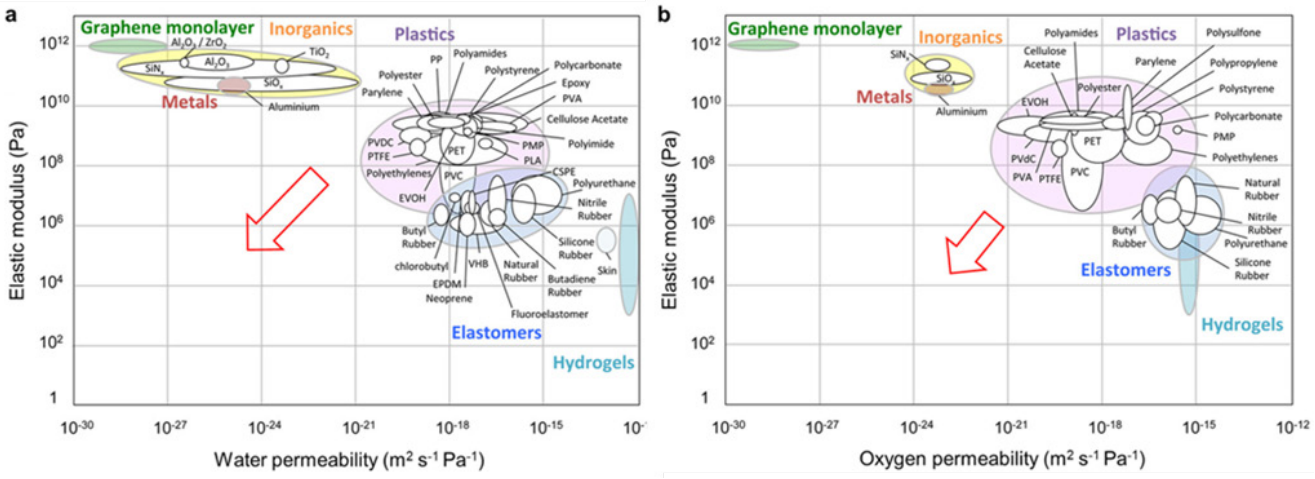


Figure 5: a Schematic illustration of PEDOT:PSS transferred CVD graphene film (PTG) as a skin electrode for electrophysiology22. b Chemical structure of PEDOT:PSS, graphene, sodium dodecyl sulfate (SDS), and bis(trifluoromethane) sulfonimide lithium salt (BSL). c Schematic illustration of the fabrication process of the double-layer stacked structure of PEDOT:PSS/graphene. Inset is a transparent PTG held on a plastic substrate. Reprinted with permission [7] , Copyright © 2018, American Chemical Society.

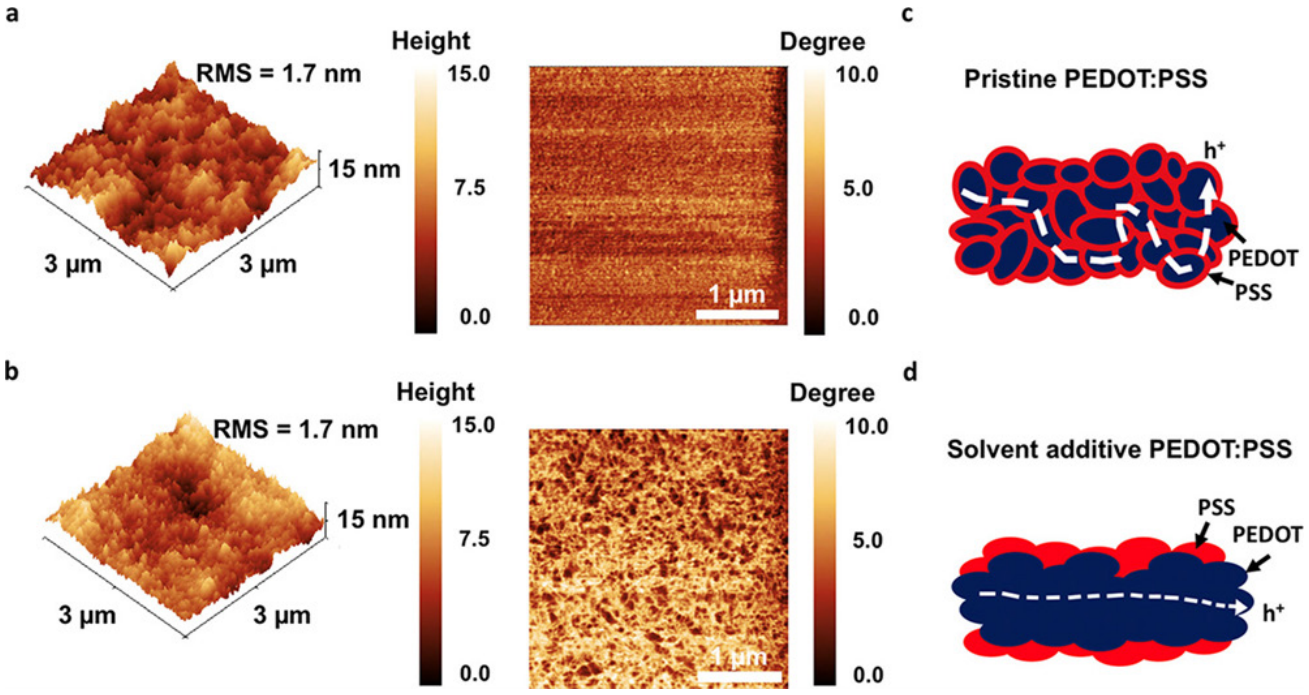


Figure 6. Morphology of the pristine PEDOT:PSS and PEDOT:PSS thin films with 5 wt % EG27. Height and phase images of printed thin films of (a) PEDOT:PSS and (b) PEDOT:PSS with 5 wt % EG obtained with tapping-mode AFM. (c) Schematic illustration of the hole transport in the pristine PEDOT:PSS thin film. (d) Schematic illustrating the PEDOT:PSS phase separation and structural rearrangement after the addition of EG. Reprinted with permission [8] , Copyright © 2021, American Chemical Society.

strategy is attractive because it preserves the electrical performance of conventional devices while maintaining the conformal contact needed for on-skin sensing; however, it also introduces stress concentration at the interface between rigid and soft regions, which remains a major source of failure. Figure 8 shows representative structural designs for stretchable interconnects in hybrid systems. A more specific mechanics problem emerges in island–bridge layouts, where rigid islands are bonded to soft substrates. Ma et al. show that this modulus mismatch generates a pronounced island effect, producing localized strain concentration near the island boundary under biaxial stretching; importantly, the normalized island size (R/L) is identified as the main parameter controlling the deformation field, with larger islands causing sharper local strain amplification[32]. These results clarify the central trade-off in flexible biosensor design: increasing rigid areas can improve functional integration, but it also raises the risk of interfacial damage and mechanical instability. This mechanics-guided view provides the foundation for evaluating how specific biosensor modalities preserve performance during real-world wear. Figure 9 visualizes the strain concentration that develops around rigid islands on a soft substrate, which shows the geometric model of an island–substrate system and the corresponding localized strain field near the island edge. It directly supports the conclusion that rigid–soft modulus mismatch governs interfacial strain concentration in island-based flexible electronics.

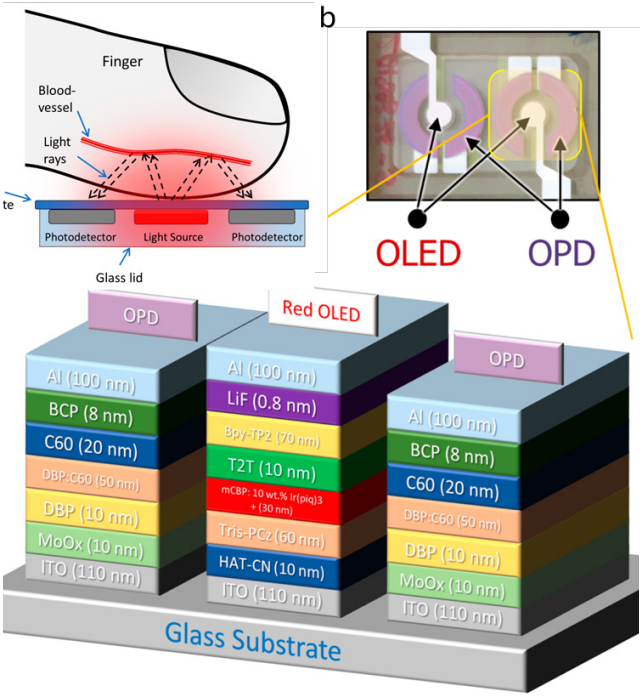


Figure 7: (a) Schematic of the acquisition of PPG signal from the reflection method. (b) The fabricated organic biosensor pulse meter. (c) A cross-section of the organic material structure of the OLED and OPD for the devices. Adopted with permission [9] , Creative Commons Attribution 4.0 (CC BY 4.0),

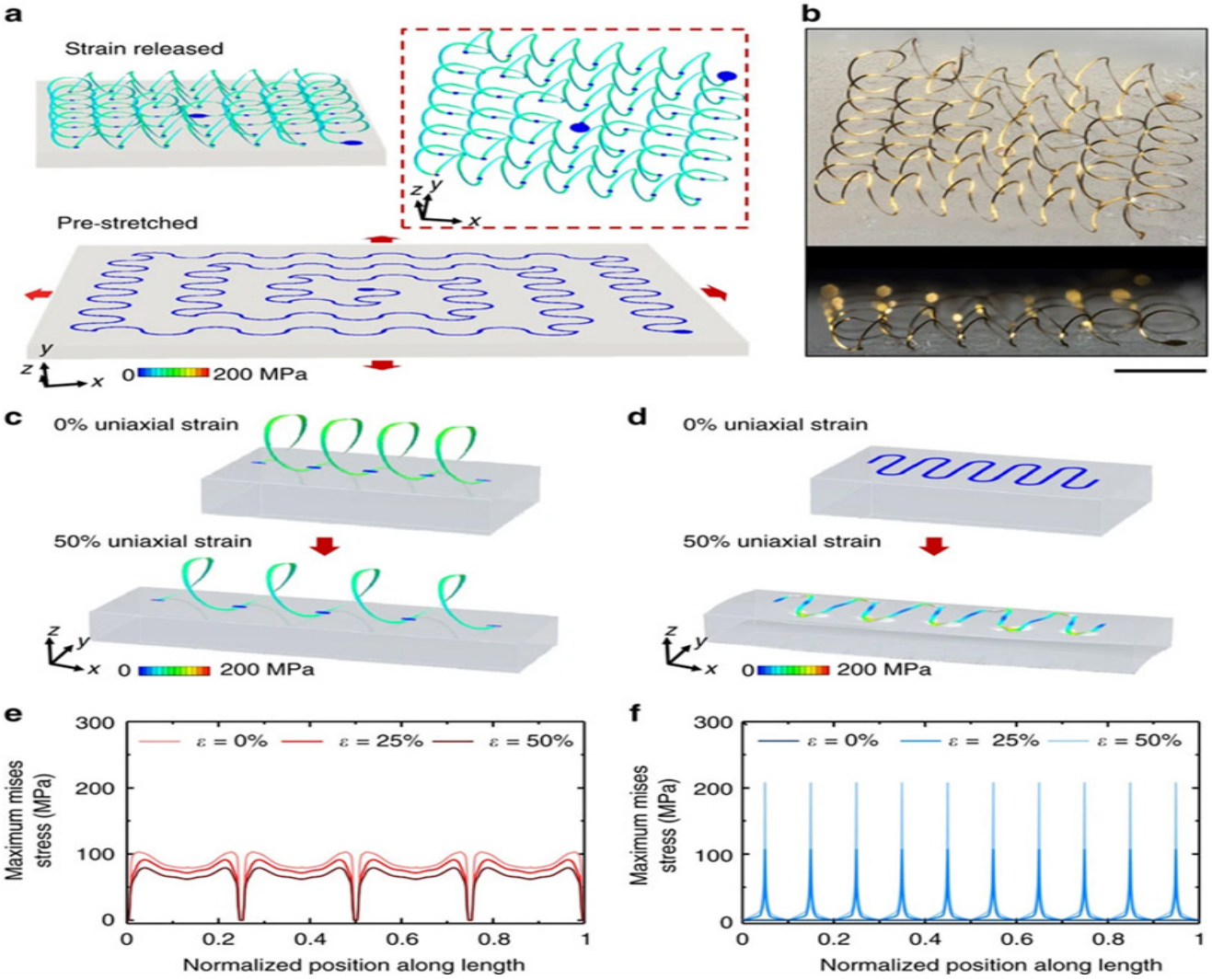


Figure 8. Assembly of conductive 3D helical coils and their mechanical properties31. (a) Process for assembly illustrated by finite element analysis (FEA). (b) Angled and cross-sectional optical images of an experimentally realized structure. FEA results for the deformations and distributions of Mises stress in a 3D coil (c) and a 2D serpentine (d) with similar geometries at 0 and 50% uniaxial strain. (e) Distribution of maximum Mises stress for each cross section along the natural coordinate normalized by the arc length, for the 3D helical coil in c, for three different levels of applied strain (0, 25, 50%). (f) Similar results for the case of the 2D serpentine in d. Reprinted with permission [10]Creative Commons Attribution 4.0 (CC BY 4.0),

4. FABRICATION AND INTEGRATION STRATEGIES

4.1 PRINTING AND ADDITIVE MANUFACTURING

Printing-based fabrication has become a major route for flexible biosensors because it enables electrodes, interconnects, and active layers to be patterned directly on compliant substrates with fewer process steps than conventional microfabrication. More importantly, the distinction among printing approaches lies not simply in the deposition method itself, but in the tradeoff, each offers among prototyping speed, throughput, material compatibility, and device reproducibility. Inkjet printing is particularly attractive for digital, maskless patterning of multiplexed sensor arrays and integrated interconnects on flexible substrates. Recent studies further indicate that advances in ink formulation and interface engineering can substantially improve adhesion, charge transfer, and long-term operational stability in fully printed wearable platforms[33, 34] By contrast, screen printing remains highly valuable for low-cost and reproducible disposable devices, although its dependence on physical screens and relatively viscous contact inks makes rapid redesign and the deposition of sensitive solution-processed materials less straightforward.

Additive manufacturing, particularly extrusion-based 3D printing, further extends this fabrication landscape by enabling custom geometries, rapid design iteration, and small- to medium-batch production. A representative example is provided by the carbon-based biosensors of Marculescu et al.,[35] which were printed on Kapton and transferred to poly(dimethylsiloxane) (PDMS) with an extrusion resolution of 100 μm, illustrating how 3D printing can support rapid customization and potential integration into wound-dressing-type platforms. At the same

time, this example also highlights broader challenges that remain across the field, including printable ink formulation, transfer fidelity, and downstream encapsulation. Overall, the literature suggests that printing-based fabrication is most advantageous when low-cost, large-area, customizable, or disposable manufacturing is required, whereas performance-critical systems still depend strongly on interface control, material optimization, and post-processing. This emphasis on direct patterning and scalable fabrication naturally leads to a second strategy: integrating high-performance ultrathin devices with soft substrates through transfer printing and lamination.

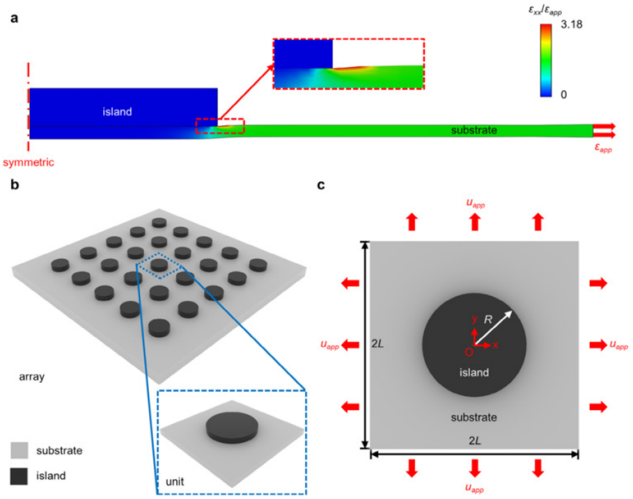


Figure 9: The geometric model of the island-substrate structure with island effect. a) Contour plot of the normalized normal strain along the x direction in the island-substrate structure (front view). b) A periodic array and a representative unit of the island-substrate structure. c) Schematic diagram of the geometric model for the island effect.[32] Reprinted with permission 11 , ©2025 Small published by Wiley VCH GmbH.

4.2 TRANSFER PRINTING AND LAMINATION

Transfer printing and lamination address a different integration challenge. Rather than patterning all functional components directly onto soft substrates, these approaches relocate ultrathin active layers or prefabricated devices onto skin-like supports while preserving device performance. A growing body of research highlights the importance of this strategy for epidermal electronics, where conformability, imperceptibility, and gentle skin coupling are as essential as electronic functionality.[36-38]

This design logic is well illustrated by the transferable e-tattoo architecture reported by Huttunen et al.,[37] in which a 30 µm breathable PDMS multilayer supports printed Ag/AgCl electrodes and encapsulated interconnects while maintaining defined openings for skin contact and exposed pads for external electronics. This approach is particularly noteworthy because it conceptualizes the entire signal transmission pathway, from the skin interface to the reusable module, as an integrated element of transfer printing design rather than a downstream assembly consideration. In parallel, Burtscher et al.[38] used temporary tattoo paper as a decal-transfer substrate for ultrathin printed organic photodiodes, showing that transfer approaches can support not only electrodes but also optoelectronic elements with sub-micrometer supporting films and high conformability. Figure 9 illustrates the multilayer architecture of e-tattoo systems and their integration onto skin, emphasizing the role of transfer printing and lamination in achieving conformal contact together with protected interconnect routing.

Overall, transfer printing is strongest when device performance depends on ultrathin geometry, heterogeneous materials, or skin-like mechanics, but its success depends on reliable release layers, lamination fidelity, and connection design. These requirements make system-level integration the next critical challenge

4.3 SYSTEM LEVEL INTEGRATION

At the system level, the performance of flexible biosensors depends not only on mechanical compliance with skin but also on reliable interfacing with signal-conditioning electronics, power supplies, and protective packaging suitable for practical use. Recent studies consistently identify the soft–hard interface as a major bottleneck, because failure often occurs not in the sensing element itself, but at the transition between ultrathin soft devices and more rigid components such as cables, circuit boards, batteries, or communication hardware. [39, 40].For connectors and interconnect routing, current strategies generally include flexible cable extension for conventional flat-flex connectors, anisotropic conductive bonding to external wiring, and direct printing of conductors from compliant sensor platforms to external contact pads. These routes differ in footprint, process complexity, and layout freedom, making connector choice application-specific rather than universal. The practical implementation of this principle can be seen in the e-tattoo platform of Huttunen et al.,[37] where exposed tattoo pads connect the skin-mounted sensor to a reusable wireless ECG recorder built on a 100 µm TPU substrate and incorporating a microcontroller, analog front-end, Bluetooth unit, and a thin coin-cell battery. As shown in Figure 10 a–b, this design makes clear that practical wearable integration begins at the epidermal interface, where electrical continuity, mechanical compliance, and module reusability must be coordinated rather than optimized separately.

A complementary integration strategy is demonstrated by Xu et al.,[41] who combined flexible tactile sensors with flexible printed circuit boards, amplifiers, antennas, batteries, and Bluetooth circuitry to realize wireless biomechanical monitoring. Their work further extends to ASIC-coupled tactile arrays and bonding-wire interconnects, highlighting that system-level performance depends not only on the softness of the sensing layer, but also on scalable assembly, reliable chip-to-substrate routing, and compatibility with established electronic packaging practices.

Packaging and power management further complete this system perspective. Across the literature, stable wearable operation requires effective encapsulation, suppression of signal drift, reliable interconnection, and practical power delivery. Accordingly, truly standalone flexible biosensors must integrate sensing, signal processing, communication, and power management within a unified system architecture rather than rely primarily on external instrumentation.

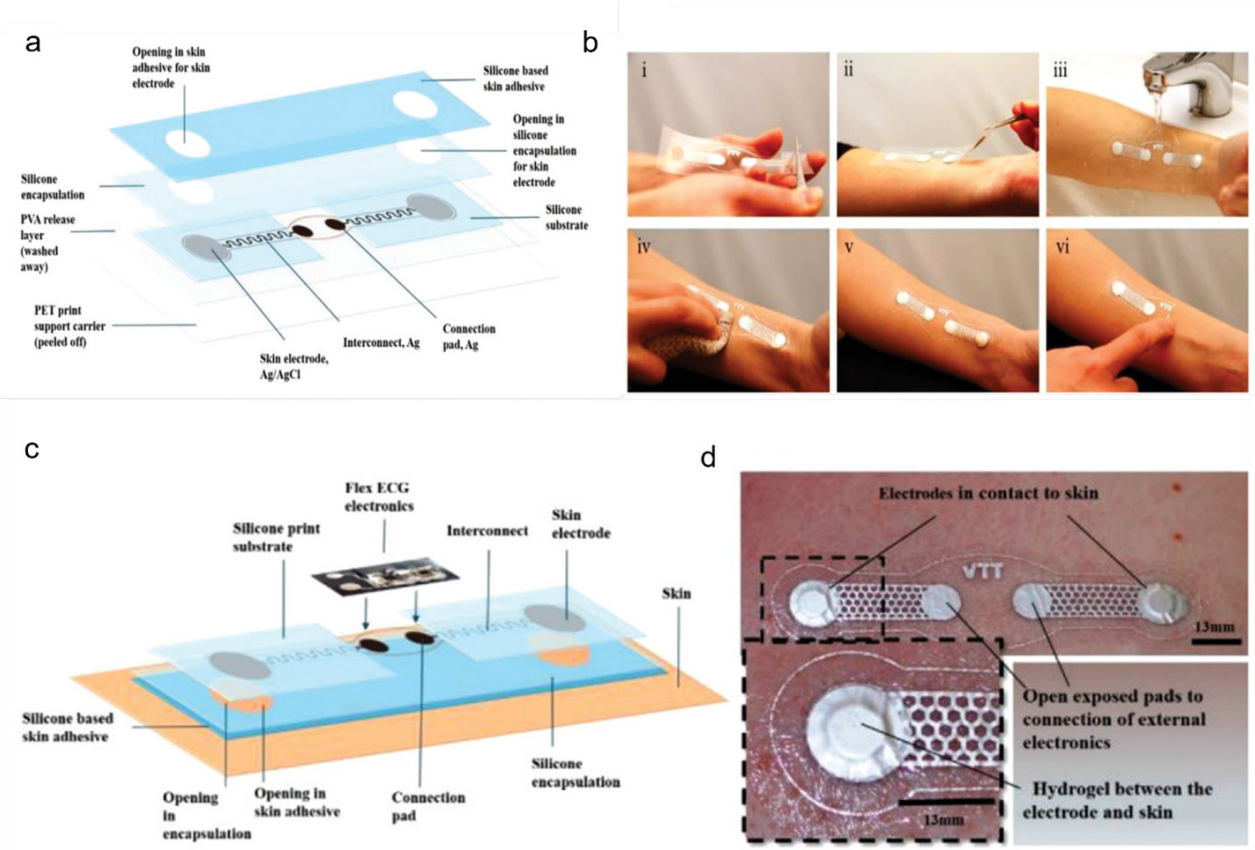


Figure 10: The operation principle of the electronic tattoo. (a) Schematic of the representative e-tattoo multilayer structure on the print-carrier substrate before release; release occurs at the PET/PVA interface. (b) Transfer sequence: (i) detachment from the carrier, (ii) placement onto skin, (iii) removal of the PVA release layer by washing, (iv) optional drying, (v) final mounting on skin, and (vi) removal from skin.(c) Schematic cross-sectional view of the e-tattoo on skin after removal of the PVA layer, with integrated ECG electronics.(d) Optical image and enlarged view of the e-tattoo mounted on human skin; the ECG electronics are omitted here for visual clarity. Adapted from Huttunen et al., [37] Advanced Materials Technologies 2022, 7, 2101496 (DOI: 10.1002/admt.202101496), licensed under Creative Commons Attribution 4.0 (CC BY 4.0). https://creativecommons.org/licenses/by/4.0/.

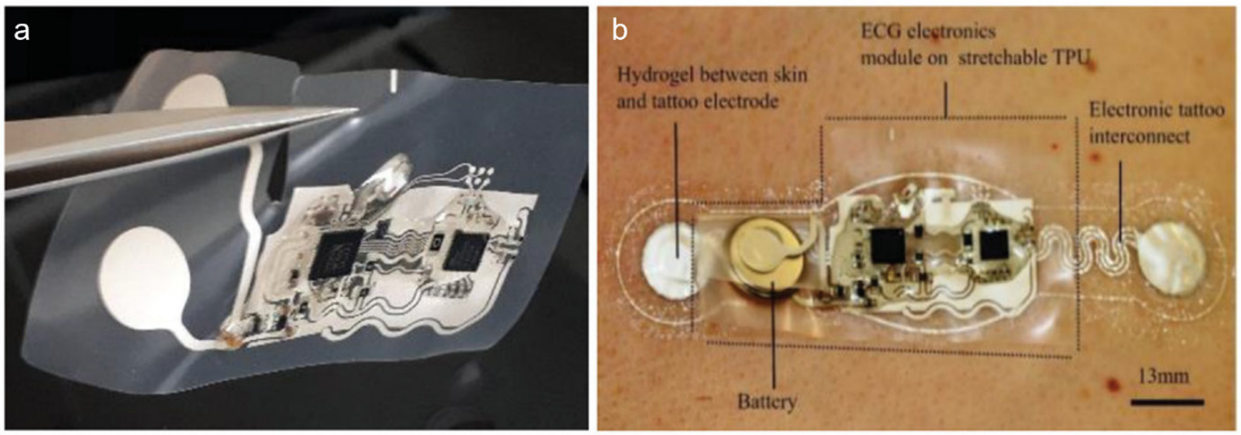


Figure 11: System-level integration of flexible biosensors for wearable health monitoring. (a) Optical image of the stretchable ECG electronics module. (b) Optical image of the stretchable ECG electronics coupled to a skin-mounted e-tattoo. Adapted from Huttunen et al., [37] Advanced Materials Technologies 2022, 7, 2101496 (DOI: 10.1002/admt.202101496), licensed under Creative Commons Attribution 4.0 (CC BY 4.0). https://creativecommons.org/licenses/by/4.0/.

5. SIGNAL PROCESSING AND MACHINE LEARNING WITH FLEXIBLE BIOSENSORS

The sensor architectures, stretchable interconnects, and fabrication strategies described in Sections 3–4 determine not only mechanical reliability but also the noise floor, artifact profile, and multimodal data quality that downstream algorithms must accommodate. Flexible biosensors introduce signal-conditioning challenges that are largely absent in rigid clinical instrumentation: motion artifacts from skin–electrode delamination, stretch-induced impedance variation across serpentine or island–bridge traces, baseline drift from conformal contact changes, and time-varying crosstalk in densely printed multimodal arrays [42, 43].These challenges, however, also create unique opportunities for AI systems that can learn sensor-specific artifact signatures and exploit co-registered multimodal streams.

5.1 CLASSICAL SIGNAL PROCESSING PIPELINES

Traditional preprocessing remains essential even when deep learning is employed for final inference. For flexible ECG patches, the canonical pipeline comprises hardware-level analog front-end filtering (0.05–150 Hz bandpass), followed by digital baseline-wander removal (typically a high-pass Butterworth or cubic-spline interpolator at 0.5 Hz), power-line notch filtering at 50/60 Hz, and motion-artifact suppression[44] .Motion-artifact rejection is particularly critical for conformal wearables: adaptive filters (LMS, NLMS, RLS) that use a co-located accelerometer or gyroscope as a reference channel remain the most widely adopted approach, although recent work has demonstrated 2-D convolutional denoising autoencoders that operate directly on spectrogram representations of corrupted ECG from flexible substrates[45] . Wavelet-based denoising (discrete wavelet transform with soft thresholding) and empirical mode decomposition (EMD) continue to offer complementary time–frequency localization advantages for non-stationary biosignals such as PPG and electrodermal activity[44] . For cuffless blood-pressure estimation, pulse-transit-time (PTT) extraction from synchronized ECG–PPG flexible arrays demands sub-millisecond temporal alignment, making clock-jitter and sampling-rate mismatch between heterogeneous printed front-ends a non-trivial preprocessing concern[7].Similarly, biochemical channels (sweat glucose, lactate) require drift compensation and temperature correction before meaningful feature extraction, underscoring the need for physics-aware preprocessing that accounts for the specific transduction mechanism and substrate deformation state[43] .

5.2 MACHINE-LEARNING METHODS

Supervised learning on flexible-sensor data has progressed rapidly from conventional classifiers (random forests, SVMs, gradient-boosted trees) to deep architectures. One-dimensional convolutional neural networks (1-D CNNs) and residual networks dominate single-lead ECG arrhythmia detection, achieving >99% accuracy on benchmark datasets when combined with attention mechanisms[46] .Recurrent architectures (LSTMs, bidirectional GRUs) remain competitive for time-series forecasting tasks such as continuous blood-pressure tracking, where temporal context across multiple cardiac cycles is essential[7] . More recently, transformer-based models have demonstrated strong performance for ECG interpretation: hybrid CNN–transformer networks capture both local morphological features and long-range dependencies, while large-scale ECG foundation models trained on more than 10 million recordings achieve expert-level diagnostic accuracy across 80 cardiovascular conditions and transfer effectively to single-lead wearable data[47, 48] . Multimodal fusion is emerging as a key advantage of flexible platforms that co-integrate ECG, PPG, temperature, and biochemical channels on a single skin-conformal patch. Attention-based cross-modal architectures and diffusion transformers can now perform signal reconstruction, denoising, imputation, and cross-modal translation across PPG, ECG, and blood-pressure waveforms, enabling robust inference even when individual channels are corrupted by motion[43, 49]. Federated learning addresses the privacy constraints inherent in wearable health data: cross-device federated autoencoder frameworks enable ECG anomaly detection without raw data leaving the sensor node, while differential-privacy guarantees further protect patient information[50, 51] . Self-supervised pretraining on large-scale unlabeled wearable recordings exemplified by PPG and ECG foundation models promises to reduce the labeled-data burden that currently limits clinical translation of flexible-sensor AI[51, 52] .

5.3 "DESIGN-FOR-AI" CONSIDERATIONS

The co-design of sensor hardware and machine-learning pipeline is critical for flexible wearables and represents a paradigm shift from the traditional sequential design approach. Several hardware–algorithm interaction pathways merit explicit consideration.

Sensor placement and modality selection:
Electrode location and inter-electrode spacing on island–bridge arrays directly govern ECG lead-field geometry and, consequently, the morphological features available to downstream classifiers. Huang et al. (2025) [53] demonstrated that AI-guided optimization of wear positioning on a flexible ECG patch significantly improved diagnostic accuracy relative to fixed-location designs. Similarly, the choice of PPG wavelength and photodetector placement on stretchable substrates determines signal-to-noise ratio across skin tones, which in turn bounds the achievable accuracy of SpO_2 and heart-rate modesl[54].

Mechanical layout and noise topology:
Serpentine interconnects and island–bridge architectures (Section 3) localize strain to geometrically designed deformation zones, producing spatially structured noise patterns that differ fundamentally from the uniform Gaussian noise assumed by most standard denoising algorithms. Stretchable in-sensor computing platforms based on organic electrochemical transistor (OECT) arrays have shown that reservoir-computing accuracy remains above 90% even at 50% tensile strain, provided the mechanical design confines deformation away from active transduction elements[55] .In contrast, fully printed sensor arrays without strain-isolation features exhibit correlated noise across channels, requiring multichannel blind-source-separation or physics-informed artifact models for effective signal recovery[56] .

Sampling schemes and on-device feasibility:

Fabrication method constrains front-end resolution and power, which directly determines model complexity. Screen-printed electrodes with thick-film interconnects typically support lower sampling rates (125–250 Hz) than photolithographically patterned thin-film counterparts (500–1000 Hz), limiting the temporal features available for morphological analysis. Quantized and pruned CNN architectures (INT8, binary-weight networks) are therefore essential for deployment on the microcontrollers commonly paired with printed flexible sensors[57] .Conversely, rigid–flex hybrid systems with ASIC front-ends permit higher-fidelity sampling and support transformer-based inference at the edge, illustrating how fabrication choices cascade into algorithm design space[58] .

Integrated device platforms:

Fully standalone stretchable systems that combine sensing, preprocessing, and adaptive ML on a single conformal platform have recently been demonstrated. Xu et al. (2023)[52] reported a hydrogel-electrode device with embedded triaxial accelerometry and on-board adaptive ML achieving >90% classification accuracy for motion and speech tasks, highlighting that end-to-end design-for-AI can substantially mitigate the data-quality challenges inherent in flexible form factors.

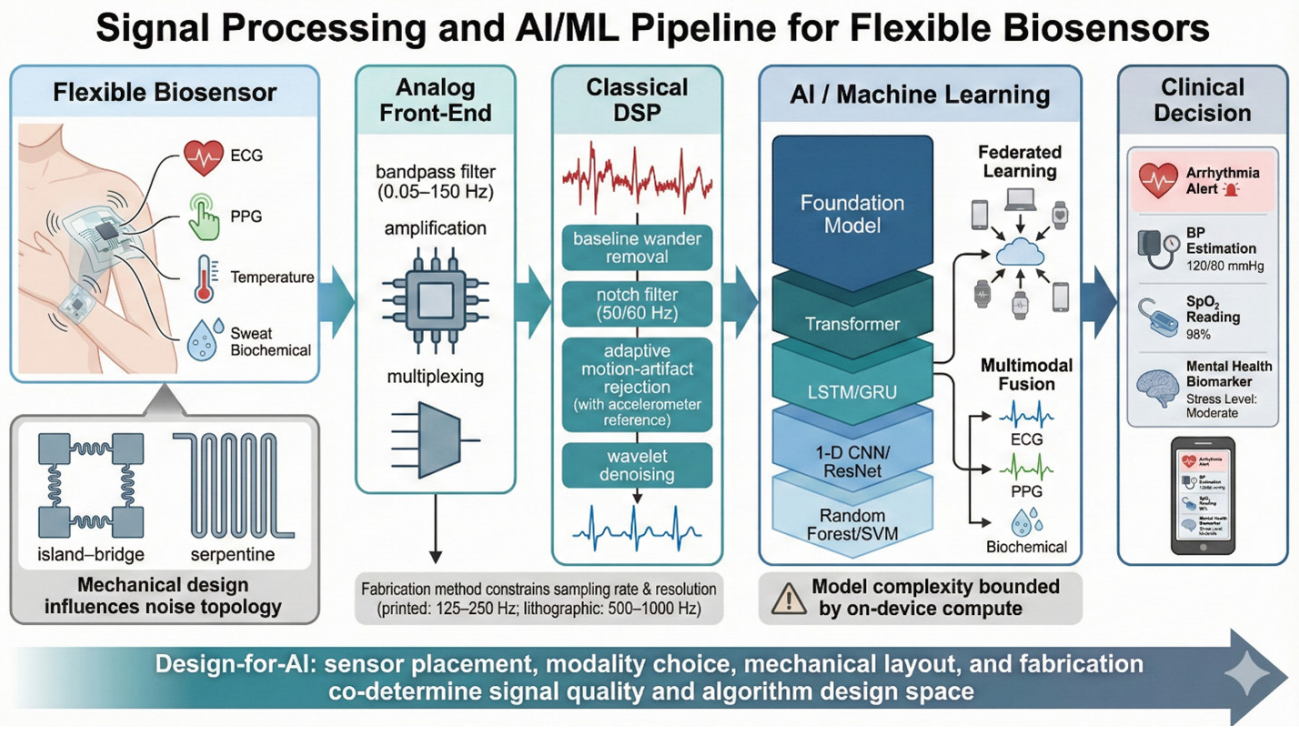


Figure 12: Signal processing and AI/ML pipeline for flexible biosensors in health monitoring. Raw biosignals (ECG, PPG, temperature, sweat biochemical analytes) acquired by skin-conformal multimodal sensor patches undergo sequential processing through four stages: (i) analog front-end conditioning, where fabrication method (printed vs. lithographic) constrains achievable sampling rate and resolution; (ii) classical digital signal processing, including baseline-wander removal, power-line notch filtering, and adaptive motion-artifact rejection using co-located inertial references; (iii) machine-learning inference, spanning conventional classifiers (RF, SVM), deep architectures (1-D CNN, LSTM, transformer), foundation models, and federated learning frameworks; and (iv) clinical decision outputs (arrhythmia detection, cuffless blood-pressure estimation, SpO_2, mental-health biomarkers). The bottom annotation highlights the design-for-AI principle: mechanical layout choices made in Sections 3–4 (island–bridge and serpentine architectures, printed vs. transfer-printed interconnects) directly shape the noise topology, artifact profile, and feature space available to downstream algorithms, thereby co-determining model accuracy, robustness, and on-device feasibility.

6. TOWARD EDGE AND NEUROMORPHIC INTELLIGENCE

6.1 CLASSICAL SIGNAL PROCESSING PIPELINES

Continuous health monitoring with flexible wearables demands real-time, low-power inference at or near the sensor node rather than dependence on cloud connectivity. Edge-AI implementations address four interrelated requirements: latency (sub-second alerting for arrhythmia or seizure), privacy (health data never leaving the device), power (microwatt-to-milliwatt budgets compatible with thin-film batteries or energy harvesters), and resilience in disconnected, disrupted, intermittent, or low-bandwidth (DDIL) environments such as rural clinics, disaster zones, and ambulatory home settings58.

TinyML frameworks—TensorFlow Lite Micro, Edge Impulse, and microTVM—enable deployment of quantized CNNs and lightweight transformers on Arm Cortex-M class microcontrollers with as little as 256 kB SRAM. Recent surveys document sub-50 ms inference

latency and fewer than 30 MB memory footprint for hybrid transformer-based ECG classifiers running on Raspberry Pi 4B, while INT8-quantized CNNs achieve clinically acceptable arrhythmia detection on sub-dollar microcontrollers paired with printed flexible ECG patches[57, 61] .Knowledge distillation—compressing a large teacher network into a student model with 10–100× fewer parameters—and structured pruning further shrink model footprints without significant accuracy loss. On-device micro-training (so-called μ-trainers) extends this paradigm by enabling personalized fine-tuning directly on the wearable, eliminating the need for cloud round-trips and improving robustness to user-specific anatomy and skin–electrode interface variability[62]. Emerging memristor-based neuromorphic accelerators offer an additional path to ultra-low-power, in-memory computation for these edge-AI biosensing workloads, with recent comparative reviews highlighting how different machine learning algorithms map onto memristive synapses for dense, energy-efficient inference at the sensor node[63].

Federated learning at the edge provides a complementary privacy-preserving pathway. In cross-device FL architectures, each wearable node trains a local model update that is aggregated centrally without transmitting raw biosignals, enabling population-scale learning from heterogeneous flexible-sensor hardware while satisfying regulatory data-residency requirements.[50, 61].

Table 1: Comparison of machine-learning approaches for flexible biosensor data. Accuracy ranges are representative values from single-lead ECG arrhythmia classification or cardiovascular diagnostics; actual performance varies with task, dataset, and sensor hardware. Edge suitability rated from * (poor) to ***** (excellent) based on combined model size, latency, and power requirements.

Method	Typical Accuracy	Latency	Model Size	Data Requirement	Edge Suitability	Key References
RF / SVM / XGBoost	85–95%	<1 ms	<1 MB	Low–Moderate (hundreds)	*****	[37,56,81]
1-D CNN / ResNet	95–99%	1–10 ms	0.5–10 MB	Moderate (thousands)	****	[46,42]
LSTM / Bi-GRU	90–97%	5–50 ms	1–20 MB	Moderate–High (thousands)	***	[7,59]
Transformer / CNN–Transformer	97–99.6%	10–100 ms	5–100 MB	High (tens of thousands)	**	[46,48]
Foundation Model (pretrained)	AUROC >0.95 (80 dx)	50–500 ms	50–500 MB	Very low (few-shot fine-tune)	* (cloud)/ ** (distilled)	[47,51]
Federated Learning (any backbone)	Comparable to centralized	Per-round: minutes	Same as backbone	Distributed (multi-device)	****	[50,51]
Diffusion Transformer (generative)	Cross-modal RMSE <5%	100 ms	50–200 MB	Very high (millions)	*	[60,49]

6.2 OPPORTUNITIES FOR NEUROMORPHIC AND IN-MEMORY COMPUTING

Biosignals acquired by flexible sensors are inherently event-driven and temporally sparse: an ECG R-peak, a PPG pulse onset, or a sweat-analyte threshold crossing each represents a discrete, information-rich event embedded in a largely quiescent baseline. This temporal sparsity aligns naturally with neuromorphic computing paradigms—spiking neural networks (SNNs), reservoir computing, and in-memory analog processing—that activate computation only in response to input events and thereby achieve orders-of-magnitude reductions in energy per inference relative to conventional von Neumann architectures[64-66] .

Reservoir computing offers a particularly compelling match for wearable biosignals classification because it requires training only a linear readout layer while exploiting the intrinsic nonlinear dynamics of a

physical substrate as the recurrent reservoir. MoS_2-based charge-trap memory devices have demonstrated real-time epileptic seizure detection via reservoir computing with sub-microwatt power consumption, while solution-processed ferroelectric memcapacitive synapses achieve energy-efficient ECG classification in a form factor compatible with printed flexible electronics[60, 67].Organic electrochemical transistor (OECT) arrays fabricated by inkjet printing on flexible substrates have been configured as wearable in-sensor reservoir-computing platforms, performing gesture recognition at >90% accuracy under 50% mechanical strain[55].

The convergence of printed neuromorphic hardware and flexible biosensing has recently yielded fully integrated prototypes[68]. Choi et al. (2025)[69] demonstrated an all-printed, chip-less wearable neuromorphic system using inkjet-printed artificial synapses for simultaneous metabolite, cardiac, and temperature monitoring; the device performed on-body sepsis-risk stratification without any silicon integrated circuit. Similarly, retrainable organic neuromorphic biosensors with on-chip learning have classified cystic fibrosis biomarkers directly from sweat without external software training[70]. These devices embody the concept of brain-like triage engines: low-power, event-responsive processors that perform clinically meaningful classification at the sensor interface and transmit only high-level alerts or compressed feature vectors, dramatically reducing communication bandwidth and battery drain in continuous monitoring scenarios[64, 71].

7. CHALLENGES AND FUTURE DIRECTIONS

Reliability and calibration drift:.

Long-term deployment of flexible biosensors is constrained by signal drift arising from biofouling, sweat accumulation, mechanical fatigue of stretchable interconnects, and progressive degradation of enzyme- or ionophore-functionalized electrodes. Recent advances in stretchable organic field-effect transistor architectures with differential readout have reduced baseline drift by up to two orders of magnitude under repeated mechanical deformation[72,80] ,while machine-learning-based drift compensation using temporal CNNs and LSTM-RNN models offers a complementary algorithmic pathway[73].Nonetheless, no current flexible platform has demonstrated drift-free operation beyond several days of continuous wear without recalibration, and self-healing or antifouling surface chemistries remain at an early research stage for wearable substrates[74].

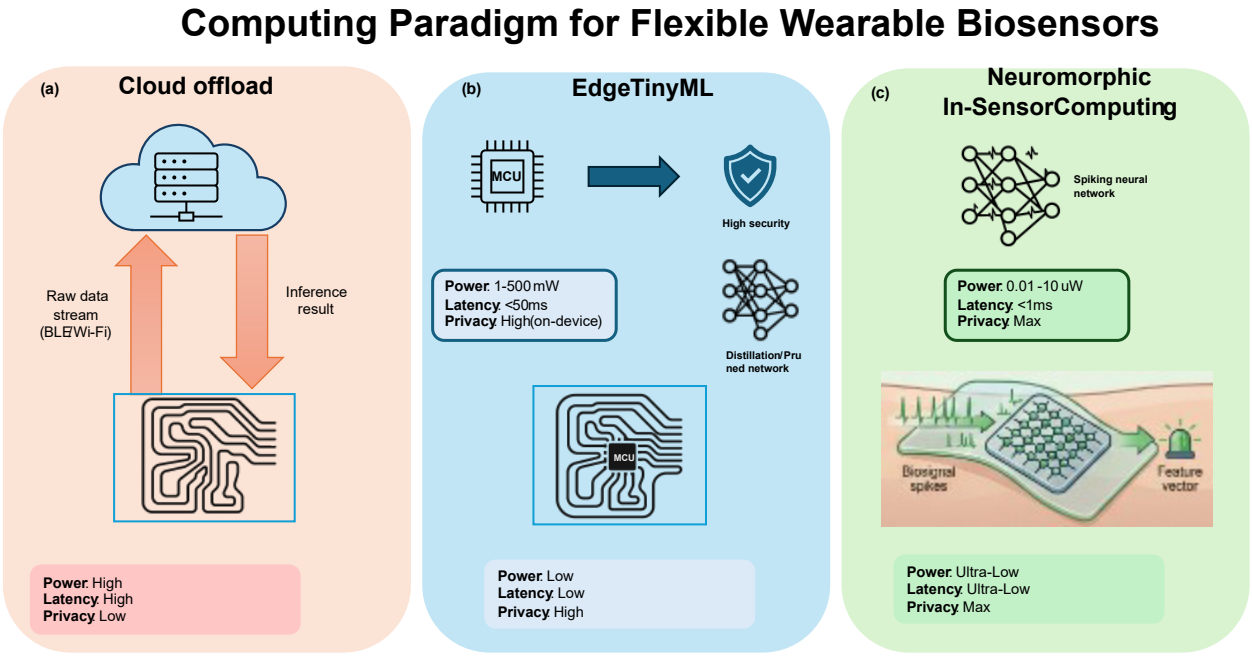


Figure 13: Comparison of computing paradigms for wearable flexible biosensor data processing. (a) Cloud offload: raw biosignals are transmitted via wireless link (BLE/Wi-Fi) to remote GPU servers for inference, offering unlimited model complexity but incurring high latency (0.1–2 s), substantial bandwidth requirements, and reduced data privacy. (b) Edge TinyML: quantized and pruned models (INT8 CNNs, lightweight transformers) execute directly on co-located microcontrollers (Arm Cortex-M class), achieving sub-50 ms latency and milliwatt-level power while retaining data on-device; model compression techniques (knowledge distillation, structured pruning) bridge the gap between cloud-level accuracy and resource-constrained hardware. (c) Neuromorphic in-sensor computing: event-driven biosignal features (R-peaks, pulse onsets, analyte threshold crossings) are processed by embedded neuromorphic substrates—spiking neural networks, physical reservoir computers (e.g., OECT arrays, MoS_2 memristors), or printed organic artificial synapses—at sub-microwatt power and sub-millisecond latency, transmitting only compressed alerts or feature vectors. The bottom strip summarizes key trade-offs across paradigms: power per inference decreases by approximately six orders of magnitude from cloud to neuromorphic, while hardware maturity follows the inverse trend, underscoring the complementary roles of each paradigm in a tiered wearable intelligence architecture.

Table 2: Comparison of computing paradigms for wearable flexible biosensor data processing. Power-per-inference values for cloud ML reflect server-side consumption and exclude sensor-node power; edge and neuromorphic values reflect total system power at the sensor node. Hardware maturity ratings reflect 2025 state-of-the-art.

Computing Paradigm	Power / Inference	Latency	Model Flexibility	HW Maturity	Flexible-Sensor Demonstration	Key Refs
Cloud ML (GPU server)	50–300 W (server-side)	0.1–2 s (incl. network)	Unlimited	High	ECG foundation model, 10M recordings; diffusion transformer for PPG/ECG/BP	[47,60]
Edge TinyML (MCU / SoC)	1–500 mW	<50 ms	Moderate (INT8, pruned)	High	Hybrid transformer on RPi4B (<30 MB); quantized CNN on flexible ECG patch	[57,61]
Spiking Neural Network	10–100 µW	1–10 ms (event-driven)	Limited (STDP, surrogate grad.)	Medium (Loihi, SpiNNaker)	ECG arrhythmia and EMG classification on neuromorphic hardware	[65,66]
Reservoir Computing (memristive)	0.1–10 µW	<1 ms	Low (linear readout only)	Low–Medium	MoS_2 reservoir for seizure detection; OECT array at 50% strain for gesture recognition	[67,55]
In-Memory Computing (crossbar)	0.01–1 µW	<100 µs	Low–Moderate (fixed weights)	Low (research-stage)	Ferroelectric memcapacitor for ECG classification; emerging IoMT memory devices	[60,71]
Printed Neuromorphic (chip-less)	<10 µW (estimated)	<10 ms	Low (task-specific)	Low (proof-of-concept)	All-printed wearable: sepsis triage with inkjet synapses; retrainable organic biosensor for CF	[69,70]

Skin-tone and anatomical variability:
Melanin-dependent optical absorption introduces systematic bias in PPG-based SpO_2 estimation, with meta-analytic evidence demonstrating clinically significant errors exceeding the 3% ARMS regulatory threshold in individuals with darker skin pigmentation[75].The largest prospective study to date (631 patients, 1,760 paired measurements) confirmed that pulse-oximeter bias varies significantly with skin tone as measured by the Monk Skin Tone Scale[76] .Mitigation strategies include multi-wavelength sensing, melanin-aware regression algorithms, and physics-based Monte Carlo correction models, yet the FDA now mandates skin-tone subgroup reporting in pulse-oximeter submissions[77].Anatomical variability—differences in subcutaneous fat thickness, vessel depth, and wrist geometry—further compounds inter-subject generalization challenges for flexible

wrist-worn and patch-type devices.

Data quality, labeling, and bias:

Wearable health AI is fundamentally constrained by training-data limitations. Ambulatory recordings from flexible sensors contain far higher proportions of corrupted, unlabeled, or ambiguously labeled segments compared with clinical-grade datasets. Demographic imbalance in publicly available wearable datasets—overrepresentation of young, healthy, light-skinned populations—propagates into algorithmic bias that disproportionately affects underserved communities [71]. Self-supervised pretraining on large-scale unlabeled wearable data (foundation models) partially mitigates label scarcity, but equitable performance across demographic subgroups requires deliberate stratified evaluation and debiasing during both data curation and model development[51].

Regulatory considerations:

The U.S. FDA's evolving framework for AI/ML-based Software as a Medical Device (SaMD) directly affects flexible biosensor products. The January 2025 draft guidance on AI-enabled device software functions introduces lifecycle management requirements including model cards, predetermined change control plans (PCCPs), and continuous real-world performance monitoring[77]. The joint FDA–Health Canada–MHRA Good Machine Learning Practice (GMLP) guiding principles and the 2024 transparency principles further mandate representative clinical study populations and disclosure of known biases[78, 79].For flexible-sensor manufacturers, compliance demands end-to-end traceability from sensor calibration through algorithm versioning to clinical outcome, a requirement that current research prototypes rarely address.

Standardized benchmarks:

The field lacks publicly available benchmark datasets that couple raw flexible-sensor signals with gold-standard clinical annotations, demographically balanced cohorts, and metadata describing sensor type, substrate material, fabrication batch, and wear conditions. Efforts such as the WildPPG dataset (216 hours of continuous real-world PPG with synchronized ECG ground truth) and the CAPTURE-24 activity-recognition corpus represent important steps, but no analogous resource exists for printed or stretchable biosensor modalities[52]. Standardized evaluation protocols that report accuracy stratified by skin tone, body-mass index, motion intensity, and sensor wear time are essential for meaningful cross-study comparison and regulatory acceptance.

Integrated outlook:

The convergence of mechanically robust flexible biosensors, data-efficient AI (foundation models, federated learning, physics-informed architectures), and neuromorphic edge hardware offers a credible pathway toward truly autonomous, skin-conformal health-monitoring systems. Realizing this vision will require coordinated advances across materials science (drift-free, biocompatible transducers), electrical engineering (ultra-low-power neuromorphic ASICs and printed synaptic devices), computer science (equitable, privacy-preserving algorithms), and regulatory science (adaptive frameworks for continuously learning devices). The design-for-AI philosophy articulated throughout this review—in which sensor architecture, fabrication process, signal conditioning, and machine-learning model are co-optimized from inception—provides the intellectual scaffold for this interdisciplinary integration.

8. CONCLUSION

The integration of artificial intelligence with flexible biosensors represents a paradigm shift toward continuous, personalized health monitoring. Realizing this potential requires a "design-for-AI" framework, wherein sensor materials, mechanical layouts, and data modalities are co-optimized to maximize downstream algorithmic efficacy. High-fidelity physiological tracking demands precise mechanical architectures to mitigate motion artifacts and maintain stable skin contact, while multimodal data fusion provides the contextual variables necessary to isolate true physiological signals from environmental noise. Furthermore, decentralizing computation through edge machine learning and neuromorphic in-sensor processing drastically reduces power consumption and latency while preserving patient privacy. Despite these advances, translating prototypes into reliable clinical tools requires overcoming substantial challenges. Further research must resolve long-term calibration drift caused by biofouling and mechanical fatigue, mitigate algorithmic biases stemming from demographically imbalanced training data, and align with rigorous regulatory frameworks. Ultimately, deploying autonomous, skin-conformal monitoring systems necessitates unprecedented interdisciplinary collaboration across materials science, electronic engineering, computer science, and regulatory fields.

REFRENCES

1. Kim, D. H.; Lu, N.; Ma, R.; Kim, Y. S.; Kim, R. H.; Wang, S.; Wu, J.; Won, S. M.; Tao, H.; Islam, A.; et al. Epidermal electronics. Science 2011, 333 (6044), 838-843. DOI: 10.1126/science.1206157 From NLM.
2. Wang, Y.; Qiu, Y.; Ameri, S. K.; Jang, H.; Dai, Z.; Huang, Y.; Lu, N. Low-cost, μm-thick, tape-free electronic tattoo sensors with minimized motion and sweat artifacts. npj Flexible Electronics 2018, 2 (1), 6.
3. Gao, W.; Emaminejad, S.; Nyein, H. Y. Y.; Challa, S.; Chen, K.; Peck, A.; Fahad, H. M.; Ota, H.; Shiraki, H.; Kiriya, D.; et al. Fully integrated wearable sensor arrays for multiplexed in situ perspiration analysis. Nature 2016, 529 (7587), 509-514. DOI: 10.1038/nature16521.
4. Ates, H. C.; Nguyen, P. Q.; Gonzalez-Macia, L.; Morales-Narváez, E.; Güder, F.; Collins, J. J.; Dincer, C. End-to-end design of wearable sensors. Nature Reviews Materials 2022, 7 (11), 887-907. DOI: 10.1038/s41578-022-00460-x.
5. Hannun, A. Y.; Rajpurkar, P.; Haghpanahi, M.; Tison, G. H.; Bourn, C.; Turakhia, M. P.; Ng, A. Y. Cardiologist-level arrhythmia detection and classification in ambulatory electrocardiograms using a deep neural network. Nature Medicine 2019, 25 (1), 65-69. DOI: 10.1038/s41591-018-0268-3.
6. Sabry, F.; Eltaras, T.; Labda, W.; Alzoubi, K.; Malluhi, Q. Machine Learning for Healthcare Wearable Devices: The Big Picture. J Healthc Eng 2022, 2022, 4653923. DOI: 10.1155/2022/4653923 From NLM.
7. Zhao, L.; Liang, C.; Huang, Y.; Zhou, G.; Xiao, Y.; Ji, N.; Zhang, Y.-T.; Zhao, N. Emerging sensing and modeling technologies for wearable and cuffless blood pressure monitoring. npj Digital Medicine 2023, 6 (1), 93.
8. Yuan, R.; Tiw, P. J.; Cai, L.; Yang, Z.; Liu, C.; Zhang, T.; Ge, C.; Huang, R.; Yang, Y. A neuromorphic physiological signal processing system based on VO2 memristor for next-generation human-machine interface. Nature Communications 2023, 14 (1), 3695. DOI: 10.1038/s41467-023-39430-4.
9. Yamamoto, Y.; Yamamoto, D.; Takada, M.; Naito, H.; Arie, T.; Akita, S.; Takei, K. Efficient skin temperature sensor and stable gel less sticky ECG sensor for a wearable flexible healthcare patch. Advanced healthcare materials 2017, 6 (17), 1700495.
10. Hao, Y.; Yan, Q.; Liu, H.; He, X.; Zhang, P.; Qin, X.; Wang, R.; Sun, J.; Wang, L.; Cheng, Y. A stretchable, breathable, and self adhesive electronic skin with multimodal sensing capabilities for human centered healthcare. Advanced Functional Materials 2023, 33 (44), 2303881.
11. Wu, W.; Li, L.; Li, Z.; Sun, J.; Wang, L. Extensible integrated system for real time monitoring of cardiovascular physiological signals and limb health. Advanced Materials 2023, 35 (51), 2304596.
12. Karolcik, S.; Ming, D. K.; Yacoub, S.; Holmes, A. H.; Georgiou, P. A Multi-Site, Multi-Wavelength PPG Platform for Continuous Non-Invasive Health Monitoring in Hospital Settings. IEEE Trans Biomed Circuits Syst 2023, 17 (2), 349-361. DOI: 10.1109/tbcas.2023.3254453 From NLM.
13. Min, S.; An, J.; Lee, J. H.; Kim, J. H.; Joe, D. J.; Eom, S. H.; Yoo, C. D.; Ahn, H.-S.; Hwang, J.-Y.; Xu, S. Wearable blood pressure sensors for cardiovascular monitoring and machine learning algorithms for blood pressure estimation. Nature Reviews Cardiology 2025, 22 (9), 629-648.
14. Liu, W.; Cheng, J.; Wu, Z.; Li, J.; Shi, W.; Yang, W.; Jin, N.; Mu, Y.; Weng, B.; Wu, J. A wearable and flexible photoplethysmogram sensor patch for cuffless blood pressure estimation with high accuracy. IEEE Sensors Journal 2022, 22 (20), 19818-19825.
15. Sel, K.; Osman, D.; Huerta, N.; Edgar, A.; Pettigrew, R. I.; Jafari, R. Continuous cuffless blood pressure monitoring with a wearable ring bioimpedance device. npj Digital Medicine 2023, 6 (1), 59.
16. Gao, W.; Ota, H.; Kiriya, D.; Takei, K.; Javey, A. Flexible electronics toward wearable sensing. Accounts of chemical research 2019, 52 (3), 523-533.
17. Ferreira, R.; Silva, A.; Nunes-Pereira, J. Current on-skin flexible sensors, materials, manufacturing approaches, and study trends for health monitoring: a review. ACS Sens. 9 (3), 1104–1133 (2024). 2024.
18. Dcosta, J. V.; Ochoa, D.; Sanaur, S. Recent progress in flexible and wearable all organic photoplethysmography sensors for SpO2 monitoring. Advanced Science 2023, 10 (31), 2302752.
19. Dong, J.; Hou, J.; Peng, Y.; Zhang, Y.; Liu, H.; Long, J.; Park, S.; Liu, T.; Huang, Y. Breathable and stretchable epidermal electronics for health management: recent advances and challenges. Advanced Materials 2024, 36 (49), 2409071.
20. Luo, D.; Sun, H.; Li, Q.; Niu, X.; He, Y.; Liu, H. Flexible sweat sensors: from films to textiles. ACS sensors 2023, 8 (2), 465-481.
21. Li, G.; Gong, Y.; Fang, S.; You, T.; Shao, R.; Yao, L.; Liu, C.; Wu, C.; Niu, J.; Lai, W.-Y. Substrate-free ultra-thin epidermal bioelectrodes with enhanced conformality and breathability for long-term physiological monitoring. Science China Materials 2024, 67 (5), 1481-1490.
22. Zhao, Y.; Zhang, S.; Yu, T.; Zhang, Y.; Ye, G.; Cui, H.; He, C.; Jiang, W.; Zhai, Y.; Lu, C.; et al. Ultra-conformal skin electrodes with synergistically enhanced conductivity for long-time and low-motion artifact epidermal electrophysiology. Nature Communications 2021, 12 (1), 4880. DOI: 10.1038/s41467-021-25152-y.
23. Shimura, T.; Sato, S.; Tominaga, T.; Abe, S.; Yamashita, K.; Ashizawa, M.; Kato, T.; Ishikuro, H.; Matsuhisa, N. A high resolution, transparent, and stretchable polymer conductor for wearable sensor arrays. Advanced Materials Technologies 2023, 8 (12), 2201992.
24. Le Floch, P.; Meixuanzi, S.; Tang, J.; Liu, J.; Suo, Z. Stretchable seal. ACS applied materials & interfaces 2018, 10 (32), 27333-27343.
25. Sun, G.; Wang, P.; Jiang, Y.; Sun, H.; Liu, T.; Li, G.; Yu, W.; Meng, C.; Guo, S. Bioinspired flexible, breathable, waterproof and self-cleaning iontronic tactile sensors for special underwater sensing applications. Nano Energy 2023, 110, 108367.
26. Tang, L.; Cheng, S.; Zhang, L.; Mi, H.; Mou, L.; Yang, S.; Huang, Z.; Shi, X.; Jiang, X. Printable metal-polymer conductors for highly stretchable bio-devices. IScience 2018, 4, 302-311.
27. Lo, L.-W.; Zhao, J.; Wan, H.; Wang, Y.; Chakrabartty, S.; Wang, C. An inkjet-printed PEDOT: PSS-based stretchable conductor for wearable health monitoring device applications. ACS Applied Materials & Interfaces 2021, 13 (18), 21693-21702.
28. Elsamnah, F.; Bilgaiyan, A.; Affiq, M.; Shim, C.-H.; Ishidai, H.; Hattori, R. Reflectance-Based Organic Pulse Meter Sensor for Wireless Monitoring of Photoplethysmogram Signal. Biosensors 2019, 9 (3),

87.
29. Aslam, N.; Zhou, H.; Urbach, E. K.; Turner, M. J.; Walsworth, R. L.; Lukin, M. D.; Park, H. Quantum sensors for biomedical applications. Nature Reviews Physics 2023, 5 (3), 157-169. DOI: 10.1038/s42254-023-00558-3.
30. Lee, B.; Cho, H.; Jeong, S.; Yoon, J.; Jang, D.; Lee, D. K.; Kim, D.; Chung, S.; Hong, Y. Stretchable hybrid electronics: combining rigid electronic devices with stretchable interconnects into high-performance on-skin electronics. Journal of Information Display 2022, 23 (3), 163-184.
31. Jang, K.-I.; Li, K.; Chung, H. U.; Xu, S.; Jung, H. N.; Yang, Y.; Kwak, J. W.; Jung, H. H.; Song, J.; Yang, C. Self-assembled three dimensional network designs for soft electronics. Nature communications 2017, 8 (1), 1-10.
32. Ma, Z.; Li, T.; Liu, X.; Wu, J.; Luo, H.; Yang, Y. Theoretical Model of the Island Effect in Flexible Electronics under Equal Biaxial Stretching. Small 2025, 21 (19), 2409632.
33. Ma, S.; Wan, Z. a.; Wang, C.; Song, Z.; Ding, Y.; Zhang, D.; Chan, C. L. J.; Shu, L.; Huang, L.; Yang, Z. Ultra sensitive and stable multiplexed biosensors array in fully printed and integrated platforms for reliable perspiration analysis. Advanced Materials 2024, 36 (24), 2311106.
34. Boček, Ž.; Zubak, M.; Kassal, P. Fully inkjet-printed flexible graphene–Prussian blue platform for electrochemical biosensing. Biosensors 2025, 15 (1), 28.
35. Marculescu, C.; Preda, P.; Burinaru, T.; Chiriac, E.; Tincu, B.; Matei, A.; Brincoveanu, O.; Pachiu, C.; Avram, M. Customizable fabrication process for flexible carbon-based electrochemical biosensors. Chemosensors 2023, 11 (4), 204.
36. Linghu, C.; Zhang, S.; Wang, C.; Song, J. Transfer printing techniques for flexible and stretchable inorganic electronics. npj Flexible Electronics 2018, 2 (1), 26. DOI: 10.1038/s41528-018-0037-x.
37. Huttunen, O. H.; Behfar, M. H.; Hiitola Keinänen, J.; Hiltunen, J. Electronic tattoo with transferable printed electrodes and interconnects for wireless electrophysiology monitoring. Advanced Materials Technologies 2022, 7 (8), 2101496.
38. Burtscher, B.; Leising, G.; Greco, F. Temporary Tattoo Approach for a Transferable Printed Organic Photodiode. ACS Applied Electronic Materials 2021, 3 (6), 2652-2660.
39. Luo, Y.; Abidian, M. R.; Ahn, J.-H.; Akinwande, D.; Andrews, A. M.; Antonietti, M.; Bao, Z.; Berggren, M.; Berkey, C. A.; Bettinger, C. J. Technology roadmap for flexible sensors. ACS nano 2023, 17 (6), 5211-5295.
40. Kim, M. S.; Almuslem, A. S.; Babatain, W.; Bahabry, R. R.; Das, U. K.; El Atab, N.; Ghoneim, M.; Hussain, A. M.; Kutbee, A. T.; Nassar, J. Beyond flexible: unveiling the next era of flexible electronic systems. Advanced Materials 2024, 36 (51), 2406424.
41. Xu, C.; Wang, Y.; Zhang, J.; Wan, J.; Xiang, Z.; Nie, Z.; Xu, J.; Lin, X.; Zhao, P.; Wang, Y. Three-dimensional micro strain gauges as flexible, modular tactile sensors for versatile integration with micro-and macroelectronics. Science Advances 2024, 10 (34), eadp6094.
42. Khan, B.; Khalid, R. T.; Masrur, M. H.; Awais, M.; Khan, B.; Khoo, B. L. Next-generation wearable ECG systems: Soft materials, AI integration, and personalized healthcare applications. Chemical Engineering Journal 2025, 170117.
43. Cheng, J.; Xue, N.; Zhou, W.; Qin, B.; Qiu, B.; Fang, G.; Sun, X. Recent Progress in Flexible Wearable Sensors for Real-Time Health Monitoring: Materials, Devices, and System Integration. Micromachines 2025, 16 (10), 1124.
44. Jia, Y.; Pei, H.; Liang, J.; Zhou, Y.; Yang, Y.; Cui, Y.; Xiang, M. Preprocessing and denoising techniques for electrocardiography and magnetocardiography: a review. Bioengineering 2024, 11 (11), 1109.
45. Ullah, H.; Heyat, M. B. B.; Biswas, T.; Neha, N. I.; Raihan, M. M. S.; Lai, D. An end-to-end motion artifacts reduction method with 2D convolutional de-noising auto-encoders on ECG signals of wearable flexible biosensors. Digital Signal Processing 2025, 160, 105053.
46. Islam, M. R.; Qaraqe, M.; Qaraqe, K.; Serpedin, E. Cat-net: Convolution, attention, and transformer based network for single-lead ecg arrhythmia classification. Biomedical Signal Processing and Control 2024, 93, 106211.
47. Li, J.; Aguirre, A. D.; Junior, V. M.; Jin, J.; Liu, C.; Zhong, L.; Sun, C.; Clifford, G.; Brandon Westover, M.; Hong, S. An electrocardiogram foundation model built on over 10 million recordings. Nejm ai 2025, 2 (7), AIoa2401033.
48. Ansari, M. Y.; Yaqoob, M.; Ishaq, M.; Flushing, E. F.; Mangalote, I. A. C.; Dakua, S. P.; Aboumarzouk, O.; Righetti, R.; Qaraqe, M. A survey of transformers and large language models for ECG diagnosis: advances, challenges, and future directions. Artificial Intelligence Review 2025, 58 (9), 261.
49. Liu, C.; Fan, H.; Kim, M.; Zhou, T.; Yang, P.; Zhao, L.; Wang, Y.; Che, Z.; Liu, C. W.; Li, B. Multimodal Wearable Biosensing Meets Multidomain AI: A Pathway to Decentralized Healthcare. Advanced Science 2026, e22900.
50. Kapsecker, M.; Jonas, S. M. Cross-device federated unsupervised learning for the detection of anomalies in single-lead electrocardiogram signals. PLOS Digital Health 2025, 4 (4), e0000793.
51. Abbas, S. R.; Abbas, Z.; Zahir, A.; Lee, S. W. Federated learning in smart healthcare: a comprehensive review on privacy, security, and predictive analytics with IoT integration. In Healthcare, 2024; MDPI: Vol. 12, p 2587.
52. Xu, H.; Zheng, W.; Zhang, Y.; Zhao, D.; Wang, L.; Zhao, Y.; Wang, W.; Yuan, Y.; Zhang, J.; Huo, Z. A fully integrated, standalone stretchable device platform with in-sensor adaptive machine learning for rehabilitation. Nature communications 2023, 14 (1), 7769.
53. Huang, X.; Yuan, Y.; Liu, J.; He, J.; Shi, Y.; Gao, S.; Wu, J.; Xu, X.; Zhang, H.; Li, P. AI-enhanced flexible ECG patch for accurate heart disease diagnosis, optimal wear positioning, and interactive medical consultation. National Science Review 2025, 12 (12), nwaf425.
54. Soumma, S. B.; Mamun, A.; Ghasemzadeh, H. AI-powered wearable sensors for health monitoring and clinical decision making. Current Opinion in Biomedical Engineering 2025, 100628.
55. Liu, D.; Tian, X.; Bai, J.; Wang, S.; Dai, S.; Wang,

Y.; Wang, Z.; Zhang, S. A wearable in-sensor computing platform based on stretchable organic electrochemical transistors. Nature Electronics 2024, 7 (12), 1176-1185.
56. Mu, G.; Zhang, Y.; Yan, Z.; Yu, Q.; Wang, Q. Recent advancements in wearable sensors: integration with machine learning for human–machine interaction. RSC advances 2025, 15 (10), 7844-7854.
57. Keivanimehr, A. R.; Akbari, M. TinyML and edge intelligence applications in cardiovascular disease: A survey. Computers in Biology and Medicine 2025, 186, 109653.
58. Xi, L.; Li, C.; Anari, M. S.; Rezaee, K. Integrating wearable health devices with AI and edge computing for personalized rehabilitation. Journal of Cloud Computing 2025, 14 (1), 64.
59. Kargarandehkordi, A.; Li, S.; Lin, K.; Phillips, K. T.; Benzo, R. M.; Washington, P. Fusing wearable biosensors with artificial intelligence for mental health monitoring: A systematic review. Biosensors 2025, 15 (4), 202.
60. Chen, Z.; Miao, Y.; Wang, L.; Fan, L.; Mandic, D. P.; Zhu, J. Versatile cardiovascular signal generation with a unified diffusion transformer. Nature Machine Intelligence 2025, 1-14.
61. Akram, M. S.; Varma, B. S.; Javed, A.; Harkin, J.; Finlay, D. Toward TinyDPFL systems for real-time cardiac healthcare: Trends, challenges, and system-level perspectives on AI algorithms, hardware, and edge intelligence. Journal of Systems Architecture 2025, 103587.
62. Huang, Z.; Yu, L.; Herbozo Contreras, L. F.; Dwivedi, G.; Kavehei, O. On-device machine learning for secure, generalizable and real-time medical data processing: on the emergence of μ-trainers. Royal Society Open Science 2025, 12 (12).
63. Dhakal, P.; Wu, X.; Kim, J. G.; Hou, A.; Wang, S. Bridging Synapses: A Comparative Review of Machine Learning Algorithms in Memristor Technology. Journal of Neuromorphic Intelligence 2024, 1 (1).
64. Jang, H.; Lee, J.; Beak, C. J.; Biswas, S.; Lee, S. H.; Kim, H. Flexible neuromorphic electronics for wearable near sensor and in sensor computing systems. Advanced Materials 2025, 37 (9), 2416073.
65. Choi, S. H. Spiking neural networks for biomedical signal analysis. Biomedical Engineering Letters 2024, 14 (5), 955-966.
66. Kim, E.; Kim, Y. Exploring the potential of spiking neural networks in biomedical applications: advantages, limitations, and future perspectives. Biomedical Engineering Letters 2024, 14 (5), 967-980.
67. Farronato, M.; Mannocci, P.; Milozzi, A.; Compagnoni, C. M.; Barcellona, A.; Arena, A.; Crepaldi, M.; Panuccio, G.; Ielmini, D. Seizure detection via reservoir computing in MoS2-based charge trap memory devices. Science Advances 2025, 11 (3), eadr3241.
68. Kim, J. G.; Liu, R.; Dhakal, P.; Hou, A.; Gao, C.; Qiu, J.; Merkel, C.; Zoran, M.; Wang, S. Heterostimuli chemo-modulation of neuromorphic nanocomposites for time-, power-, and data-efficient machine learning. Matter 2024, 7 (3), 1230-1244.
69. Choi, Y.; Jin, P.; Lee, S.; Song, Y.; Tay, R. Y.; Kim, G.; Yoo, J.; Han, H.; Yeom, J.; Cho, J. H. All-printed chip-less wearable neuromorphic system for multimodal physicochemical health monitoring. Nature communications 2025, 16 (1), 5689.
70. Van Doremaele, E.; Ji, X.; Rivnay, J.; Van De Burgt, Y. A retrainable neuromorphic biosensor for on-chip learning and classification. Nature Electronics 2023, 6 (10), 765-770.
71. Baek, Y.; Bae, B.; Shin, H.; Sonnadara, C.; Cho, H.; Lin, C.-Y.; Mu, Y.; Shen, C.; Shah, S.; Wang, G. Edge intelligence through in-sensor and near-sensor computing for the artificial intelligence of things. Npj Unconventional Computing 2025, 2 (1), 25.
72. Zhao, C.; Park, J.; Maulà, D.; Yuan, Y.; Zhong, D.; Wang, W.; Liu, Q.; Xu, C.; Zheng, Y.; Mow, R. K. Skin-like drift-free biosensors with stretchable diode-connected organic field-effect transistors. Nature Electronics 2025, 8 (10), 981-993.
73. Lee, K.; Gul, O.; Kwon, Y.; Jeong, J.; Cho, S.; Ahn, J.; Yu, J.; Kim, C.; Lee, D.; Han, H. Smarter Sensors Through Machine Learning: Historical Insights and Emerging Trends across Sensor Technologies. Advanced Functional Materials 2025, e19859.
74. Rivera, P.; Della Pelle, F.; Stonyte, J.; Martins Antunes de Melo, W. d. C.; Abouhagger, A.; Pauliukaite, R. Overcoming Challenges in Electrochemical Sensing: Toward Continuous Monitoring. ACS sensors 2025, 10 (12), 9183-9202.
75. Singh, S.; Bennett, M. R.; Chen, C.; Shin, S.; Ghanbari, H.; Nelson, B. W. Impact of skin pigmentation on pulse oximetry blood oxygenation and wearable pulse rate accuracy: systematic review and meta-analysis. Journal of Medical Internet Research 2024, 26, e62769.
76. Hendrickson, C. M.; Lipnick, M. S.; Chen, D.; Chen, D.; Law, T. J.; Pirracchio, R.; Feiner, J. R.; Behnke, E.; Chou, Y.; Elmankabadi, S. EquiOx: A Prospective study of pulse oximeter bias and skin pigmentation in critically-ill adults. medRxiv 2025, 2025.2010. 2006.25337217.
77. Mehta, V.; Komanduri, A.; Bhadouriya, R. S.; Mehta, V.; Johnson, M. D.; Shrestha, P.; Nikolov, M.; Jain, B.; Shah, N.; Schulman, K. Evaluating transparency in AI/ML model characteristics for FDA-reviewed medical devices. npj Digital Medicine 2025, 8 (1), 673.
78. FDA, U. Artificial Intelligence-Enabled Device Software Functions: Lifecycle Management and Marketing Submission Recommendations. Draft Guidance for Industry and Food and Drug Administration Staff.[Docket No. FDA-2024-D-4488] URL: https://www. fda. gov/media/184856/download, Last accessed: Apr 2025, 18.
79. Food, U.; Administration, D. Good machine learning practice for medical device development: guiding principles. FDA webpage 2021.
80. Liu, Ruochen, et al. “Neuromorphic properties of flexible carbon nanotube/polydimethylsiloxane nanocomposites.” Advanced Composites and Hybrid Materials 6.1 (2023): 14.
81. Wu, X., Dhakal, P., Kim, J. G., Hou, A., & Wang, S. (2024). Transition metal dichalcogenides-based memristors for neuromorphic electronics. Journal of Neuromorphic Intelligence, 1(1).

COMPETING INTERESTS

The authors declare that they have no known competing financial interests or personal relationships that could have appeared to influence the work reported in this paper.

ACKNOWLEDGMENTS

The authors are grateful for the funding support from Texas A&M University